A Study of Polycarbonate / Poly (butylene terephthalate) Compounding in a Twin Screw Extruder

by

Md. Hasan Tareque

A thesis

presented to the University of Waterloo

in fulfillment of the

thesis requirement for the degree of

Master of Applied Science

in

Chemical Engineering

Waterloo, Ontario, Canada, 2009

I hereby declare that I am the sole author of this thesis. This is a true copy of the thesis, including any required final revisions, as accepted by my examiners.

I understand that my thesis may be made electronically available to the public.

ABSTRACT

In this work, the compounding of polycarbonate (PC) / poly-butylene terephthalate (PBT) blends was studied for the purpose of improving quality of products with reduced wastage and finally to satisfaction of end users. The effect of material rheological characteristics and processing conditions on compounding of PC /PBT was investigated through statistical experiments carried out on a 58 mm twin-screw extruder at SABIC Innovative Plastics Limited (formerly GE Plastics Limited) in Cobourg, Ontario.

Melt Volume-Flow Rate (MVR) is the most commonly used property to monitor the quality of products of PC/PBT blends. The MVR was studied with different sampling times and correlations between product properties (melt flow) and processing conditions (screw speed, flow rates) were discussed.

The rheological behavior of PC/PBT blends was investigated by dynamic and capillary rheometers. The effects of processing conditions (screw speed, feed rate) on viscosity were measured and it was found that the Cox-Merz rule is not valid for PC/PBT blends.

The change of morphology of PC/PBT blends was observed under a scanning electron microscope (SEM) by using different types of samples. Those samples were (i) PC/PBT blends pellets, (ii) PC/PBT blend samples, but collected after completing the rheological tests in the parallel plate rheometer, and (iii) PC/PBT blend samples, but collected after completing the rheological tests in the capillary rheometer. There was evidence that the samples collected after completing the tests in the parallel and capillary rheometer might be degraded due to temperature and time.

ACKNOWLEDGEMENTS

First and foremost, I express my gratitude to my supervisor, Prof. Costas Tzoganakis, for his guidance, suggestions and support. He is an excellent supervisor with impressive personality and responsibility. His enthusiasm and integral view on research, not only greatly contributed to the quality of this work, but also helped me become a better professional.

I would like to thank the members of our research group, especially Dr. Shuihan, Estanislao and Mohammad for their help with a variety of tasks.

I want to express my thanks and appreciations to the SABIC Innovative Plastics at Cobourg Plant, ON, Canada, especially Mr. Paul Van Laren and Mr. Daniel Ross, for providing the materials, equipment, machinery, facility, financial and technical support for completion of this work.

I would lastly like to thank my parents, family and friends, for their inspiration, love and continuing support. Most of all, I thank my wife, Sharmin who has been a source of strength and motivation of success. Also thanks to my son, Farabi and daughter, Farah for their love and affection.

TABLE OF CONTENTS

LIST OF FIGURES

LIST OF TABLES

Chapter 1
INTRODUCTION

Polymer blends offer an important route toward the development of new desired properties of materials. They represent one of the most attractive techniques to generate materials with unique combination of properties not available in a single polymer. If a polymeric material can be generated /developed at a lower cost with properties meeting specifications, then manufacturers would rather use it to remain competitive. Blending allows for the beneficial properties of two or more polymers to be combined in one material while shielding their mutual drawbacks.

Blends of poly (butylene terepthalate) (PBT) and polycarbonate (PC) materials are of commercial interest because of their potential in combination. The semi-crystalline PBT provides chemical resistance and thermal stability, while PC provides impact resistance, toughness and dimensional stability at elevated temperatures. Blend properties can be tailor-made by changing the percentage of PBT and PC in their blends. Most polymers are mutually immiscible from a thermodynamic standpoint since entropic contribution to the free energy of mixing is negligible. Most commercial polymer blends are multiphase systems.

In PC/PBT blends, the PC and the PBT are physically mixed involving transesterfication which results in the formation of PC-PBT co-polyesters. To control or prevent the transesterification reaction, some additives may be used. Also, some special additives may be used to serve as compatibilisers or as impact modifiers.

Twin screw extruders (TSE) are normally used for compounding of PC and PBT. Modular intermeshing TSEs have been considered the most important machines for

continuous melt compounding. Co-rotating and counter-rotating are two classes of intermeshing TSEs. Co-rotating TSEs have self wiping screw designs that enable them to avoid the build-up of deposits and they have been more widely used than counter-rotating intermeshing TSEs in compounding applications.

During polymer compounding, the blend components are transported and mixed along the axial direction of an extruder which consists of partially and completely filled sections of screw. Generally, PC and PBT are fed through two separate gravity hoppers into a TSE. The rotating action of the screws contributes in producing a homogeneous melt blend which is pumped through a manifold hanger die. At the die exit, the melted material is cooled in a water trough and subsequently goes through pelletizing, drying, screening, packaging and shipping to customers.

Polymer blending has been one of the most important areas of research and development in polymer processing in the past few decades. There are numerous publications addressing various topics in this area. In chapter 2 of this dissertation, a review is provided with emphasis on PC and PBT blends. In the first section of chapter 2, properties, rheology, morphology and applications of PC/PBT blends are overviewed. In the second section of chapter 2, compounding of PC/PBT blends in TSE as well as processing and diagnostics topics are discussed.

PC/PBT blends must have acceptable properties for customers or end users. Melt Volume-Flow Rate (MVR) or Melt Flow Index (MFI) is the most common quality index which characterizes the flow behavior of polymer melts with a single number. Normally, MVR is measured offline using a MVR indexer located in a quality control laboratory, however a few manufacturing companies use on-line measurements. Knowing the MVR of a polymer is vital to anticipating and controlling its processing. It is an assessment of average molecular mass and is an inverse measure of the melt viscosity.

Generally, higher MVR polymers are used in injection moulding, and lower MVR polymers are used with blow moulding or extrusion processes.

In chapter 3, the experimental procedures including design of experiments, materials and equipment used along with characterization of PC/PBT blends are presented. The melt volume-flow rate (MVR), dynamic (parallel plate) rheometry, capillary rheometry and scanning electron microscopy (SEM) measurement procedures and observations are described in the characterization section.

The results of melt volume-flow rate (MVR), dynamic (parallel plate) rheometry, capillary rheometry and scanning electron microscopy (SEM) are discussed in chapter 4. The dynamic response of PC/PBT blends is presented in section 4.2 of this chapter. In section 4.3, the validity of the Cox-Merz rule for PC/PBT blends is discussed. The morphology of PC/PBT blend pellets and that of samples collected from the parallel plate and capillary measurements are presented and discussed in section 4.4.

Finally, the conclusions of this research work are summarized in chapter 5 along with recommendations for future research directions.

Chapter 2
LITERATURE REVIEW

Polymer blending has been one of the most important areas of research and development in polymer science in the past few decades. Judging from the number of publications in this area, it continues to maintain a prominent position. In this chapter, a review is provided focusing on polycarbonate (PC) / poly(butylene terephthalate) (PBT) blends. In the first section, properties, morphology, rheology and applications of PC/PBT blends are overviewed. In the second section, compounding of PC/PBT blends in twin-screw extruders (TSE) as well as processing and diagnostics topics are discussed.

2.1 PC/PBT Blends

Polymer blends are mixtures of at least two polymers and/or copolymers comprising more than 2 wt% of each macromolecular component [1]. Polycarbonate (PC) and poly (butylene terephthalate) (PBT) are important commercial engineering polymers, each of them providing superior performance in a variety of applications. PC is an amorphous polymer and is characterized by its dimensional stability, transparency, flame resistance, high impact strength, and a very wide range of service temperature. However, PC has some shortcomings, such as poor solvent resistance, low fatigue strength, and high melt viscosity. PBT is a semicrystalline polymer with good chemical resistance, electric insulation, and processability. The PC/PBT blends can inherit the toughness of PC and the chemical resistance of PBT, and are available commercially [2]. The blend has high ductility, toughness, and the dimensional stability and low shrinkage of polycarbonate as well as the stress-crack resistance and gasoline resistance of the semi-crystalline PBT. Blends of PC and PBT show a complex morphology and exhibit partial miscibility of PC and PBT. Stabilization of the morphology and preventing continuous randomization by ester exchange are some of the important characteristics of these blends. Critical

inventions involve such discoveries that combine properties such as high impact strength, flow, and solvent stress crack resistance [3].

In general, for homopolymers and polymer blends, the molecular weight influences the impact toughness and the viscoelastic properties such as the tensile modulus and, thus the toughness of the material [4]. The mechanical properties of PC/PBT blends such as tensile strength and low temperature falling weight impact strength tend to deteriorate slightly when the number of extrusion times increases, but if the process is strictly controlled, recycling of this blend would be acceptable [5].

PBT and PC form semicompatible blends and the presence of PC affects the crystallization behavior and crystalline morphology of PBT. Crystallization of PBT is largely hindered by the presence of PC in their blends and the rate of crystallization is found to decrease with increasing level of PC [6]. Wahrmund et al. [7] studied melt blends of bisphenol A polycarbonate (PC) with PBT by differential thermal analysis (DTA) and dynamic mechanical behavior to determine their state of miscibility. Both techniques showed multiple glass transition temperatures indicative of incomplete miscibility in the amorphous phase. They demonstrated that there are amorphous phases containing both components, i.e., partial miscibility of the PC-PBT system.

Sanchez et al. [8] showed that the PC/PBT blends, although transparent in the melt state and mostly in the solid state, are partially miscible blends. They are composed by a PC-rich phase, an amorphous PBT-rich phase, and a crystalline PBT phase. The crystalline phase increases in volume when heated using PBT crystallized from both amorphous phases. Lee et al. [9] examined the phase behavior of PC/PBT blends by dynamic mechanical testing. They demonstrated that the blends of PC/PBT show two distinct relaxation peaks, indicating immiscibile behavior. Marchese et al. [10] analyzed PBT/PC samples, obtained through reactive blending with titanium (Ti) and samarium (Sm) based

catalyst, for determining a correlation between the chemical architecture, crystallizability, and miscibility. They showed that the samples have complete miscibility.

Pompe and Haubler [11] postulated that the miscibility of polycarbonate PC and poly(butylene terephthalate) PBT is controversially discussed in the literature. Partial miscibility has been generally found in melt blends of the two polymers. However, in solution cast blends they were found to be immiscible. It is known that the transesterification takes place in the melt and co-polyesters formed by the transesterification change the compatibility of PC and PBT.

The three possible mechanisms for the PC/PBT transesterification are suggested by Devaux and co-workers [12]. The exchange reaction can result either from an alcoholysis between an –OH terminated polycondensate (PC or PBT) and another macromolecular species (PBT or PC) or from an acidolysis reaction involving carboxyl terminated PBT. The transesterification can also proceed via a direct reaction between PBT unit and a PC group. The exact mechanism of the exchange reaction between PC and PBT was assessed by the study of model reactions. They concluded that the main process is that of direct transesterification. Wilkinson and Tattum [13] studied the crystallization behavior of PBT and a 50/50 PC/PBT blend with added transesterification catalyst using differential scanning calorimetry (DSC) and synchrotron small angle X-ray scattering (SAXS) / wide angle X-ray scattering (WAXS). They demonstrated that PBT crystallization was inhibited in the blend by both the presence of PC and transesterification. Also, increasing transesterification resulted in a progressive reduction in the melting and crystallization temperature and degree of crystallinity. They postulated that transesterification also induced a significant change in blend morphology.

Tattum et al. [14] formed a series of 50:50 PC/PBT blends via reactive melt blending in a torque rheometer. In their work, a controlled degree of transesterification between the

two homopolymers was initiated by the incorporation of an alkyl titanium catalyst during melt blending and finally quenching by the addition of a transesterification inhibitor. They discussed that as the degree of transesterification increased, the composition of the blends became increasingly complex, comprising of mixtures of the homopolymers and various AB-type copolymers of PC and PBT, resulting in significant changes in their thermal behavior. Also, a corresponding transformation in the morphology of the blends was observed due to the formation of increasing concentrations of co-polyesters. Hopfe et al. [15] studied melt blends of PC and PBT which were characterized for their transesterification and crystallization behavior using Fourier transform infrared spectroscopy (FTIR) as well as nuclear magnetic resonance (NMR) spectroscopy and differential scanning calorimetry (DSC). They suggested that the transesterification can be analyzed by FTIR spectroscopy using certain spectral features.

Sanchez [16] studied the aging of a PC/PBT blend with and without pigment by natural and accelerated methods. He analyzed tensile and impact properties and melt flow index was evaluated before and after aging, and also after recycling. He showed that the rupture elongation of the recycled material was very good, showing the recycling potential of this material. He suggested that tensile modulus and tensile strength were not affected by the processes to which the blend was submitted. He concluded that the impact strength of the recycled material showed a decrease after aging.

Utracki [17] suggested that most polymer blends are immiscible and need to be compatibilized. The compatibilization must accomplish: (i) optimization of the interfacial tension, (ii) stabilize the morphology against high stresses during forming, and (iii) enhance adhesion between the phases in the solid state. Compatibilization is accomplished either by addition of a compatibilizer or by reactive processing. His review focused on three aspects: description of the interphase, compatibilization by addition and

reactive compatibilization. He pointed out that the compatibilization methods can be divided into two categories:

a) By addition of: (i) a small quantity of a third component that is miscible with both phases (cosolvent, e.g., phenoxy), (ii) a small quantity of copolymer whose one part is miscible with one phase and another with another phase (e.g., 0.5 to 2 wt% of tapered block copolymer), (iii) a large amount of a core-shell, multi-purpose compatibilizer-cum-impact modifier.

b) By reactive compatibilization, which uses such strategies as: (i) trans-reactions, (ii) reactive formation of graft, block or lightly crosslinked copolymer, (iii) formation of ionically bonded structures, and (iv) mechano-chemical blending that may lead to chains' breakage and recombination, thus generation of copolymers (even at liquid nitrogen temperature).

Utracki [17] also showed that the reactive compatibilization (RC) engenders a thick interphase that results in high stability of morphology during the forming stage (e.g., during injection molding under high stress and strain), but it increases the viscosity. In some cases, as for example in PC/PBT blends, transesterification seems to be the easiest compatibilization strategy. However, since PBT crystallinity is of utmost importance, the method is neither easy to control nor of great advantage.

Mishra and Venkidusamy [18] characterized blends of PC with PBT using density measurements, DSC, IR, and TGA. They suggested addition of PBT increases the density values of blends linearly. Also, all the blends showed a single glass transition temperature, indicating the miscibility of two polymers in the amorphous phase. They discussed that with more than 6% addition of PBT to PC, PBT crystallizes as per its own crystal structure and the addition of 4% PBT to PC improves the thermal stability at

higher temperature compared to pure PC. Also, IR studies showed that addition of PBT improves the intermolecular forces in PC. Pesetskii et al. [19] showed that processes of phase separation in blends consisting of PC and PBT can cause variations in properties of both the amorphous and crystalline phases. They postulated that adhesion interaction between phases in the blend becomes weaker between the glass transition temperatures (Tg) of PBT and PC. They demonstrated that over the temperature range where interphase interactions occur and two components are in the glassy state, the blend is not impact resistant. Over the temperature range between Tg of PBT and Tg of PC, the blends become impact resistant materials because of the energy of crack propagation in the PBT amorphous phase.

Functional group containing MBS (graft terpolymer made from methyl methacrylate(M), butadiene(B) and styrene(S)) impact modifiers for the PC/PBT alloy were synthesized and characterized by Tseng and Lee [20]. They proposed that the functional group was used to improve the adhesion between the MBS and the PC/PBT alloy. Their results showed that the layer composition of the MBS exhibited a significant effect on the impact strength.

Reekmans and Nakayama [21] studied the mechanical reinforcement and the molecular structure development upon deformation of the blend PC and PBT. They showed that elastic modulus increases with the extension ratio for all compositions and temperatures and that blends with 25 - 40 wt % of PC have higher elastic modulus at low temperature than pure PBT. Also, crystallinity increases with extension ratio and is relatively smaller with increasing PC content.

Delimoy et al. [22] studied the crystallization of PC/PBT blends at low undercoolings ($<6^{0}$C) in isothermal conditions by rapidly cooling samples from the melt. On the basis of their studies, original mechanisms of crystallization were proposed. The main feature

of these mechanisms is the slowness of the PBT crystallization when it is finely dispersed and this behavior is attributed to a low nucleation density. They argued that crystallization is thought to result from a homogeneous PBT nucleation which becomes effective at such high undercoolings. This is followed by a very rapid growth of the crystals. Also, Bennekom et al. [23] postulated that the phase behavior is strongly dependent on blending and cooling conditions in blends of an amorphous polymer and a semi-crystalline polymer. In the case of partial or complete miscibility of the components in the molten state, the cooling rate and kinetics of non-isothermal crystallization will influence the final extent of phase separation at room temperature.

Hobbs et al. [24] discussed the partial melt miscibility of the PC/PBT system. They showed that among the unique morphological features of PBT/PC blends are the consistent isolation of the core/shell impact modifier (IM) in the PC phase, and crystallization and phase separation of the PBT from the partially miscible PBT/PC melt on slow cooling. Nabar and Kale [25] studied the miscibility and rheological behavior of PC/PBT blends. They suggested that the rheology of PC/PBT blends seems to show systematic variation with time of mixing and same result showed DSC data also. However, for PC/PBT blends, the processing time in an extruder and residual catalyst present in the commercial sample cause sufficient degree of transesterfication. In their work, the blends were mixed for different time periods for rheological studies. They suggested that as the mixing time is increased, the blends show decrease in viscosity.

Wu et al. [26] prepared PBT/PC blends with different interfacial adhesion strength by melt blending of the PBT and PC together with in situ formed PBT/PC copolymers. They showed that the enhanced interfacial adhesion can effectively transfer the applied stress from one phase to the other, reduce the flaws in the material and result in improved yield strength, elongation at break and Young's modulus. They demonstrated that fracture toughness of the blends increases with the reactive extrudate (RE) content.

Bai et al. [27] investigated the mechanical properties and morphology of PBT/PC/PTW (poly(ethylene-butylacrylate-glycidyl methacrylate)) blend. They showed that adding PTW (poly-ethylene–butylacrylate–glycidyl methacrylate) to a brittle PBT/PC (50/50) blend resulted in decreased tensile strength, flexural strength and flexural modulus, and increased the elongation at break and impact strength.

Hobbs et al. [28] carried out DSC measurements on a number of PBT/PC blends prepared by melt compounding and solution casting from hexafluoroisopropanol (HFIP). Their results clearly indicate that appreciable mixing of the two polymers takes place in the melt phase whereas complete separation is observed in cast films. The failure of the casting procedure to mimic the melt blending results is related in part to liquid-liquid phase separation and to crystallization of both polymers from the casting solvent.

The linear viscoelastic oscillatory shear properties of a PC and PBT, 60/40 by weight, blend and its nanocomposites with various concentrations of organically modified organoclay and clay surface treatment were studied by Depolo et al. [29]. They argued that the decrease in properties is attributed to a decrease in molecular weight. They observed a relatively small decrease in Tg and attributed it to increased compatibility.

The rheological behavior of materials is very complex, and polymers are usually more complex than alternative materials of construction [30]. A parallel plate rheometer has been developed for the study of nonlinear viscoelastic phenomena in molten plastics. By making use of a novel shear stress transducer, the effects of instrument friction and edge phenomena on the stress determination are eliminated. This makes possible the study of the response of a melt to large, transient deformations involving large shear rates [31].

The rheological behavior of molten polymers is of prime importance as it relates to their microstructure and governs their processing characteristics [32]. Rotational rheometers,

specifically cone-plate, parallel plate, and sliding plate rheometers are routinely used to characterize the linear viscoelastic properties of polymer melts. Small amplitude oscillatory shear experiments are employed to measure the storage (*G'*) and loss moduli (*G"*), which are related to the elastic and viscous character of the material, respectively, and the complex viscosity (η^*) as functions of angular frequency (ω) [33].

A well-known empiricism in the rheology of polymer melts is the Cox-Merz rule, which relates the linear dynamic moduli as functions of frequency to the steady shear flow viscosity as a function of shear rate. The Cox-Mexz [34] rule states that the (steady) viscosity versus shear rate curve is virtually identical to the dynamic viscosity versus frequency curve. It is valid for most common polymers. Since it is easier to get the dynamic data over a very wide range of frequencies, it is used extensively in industry.

Scanning electron microscopy (SEM) is widely used to elucidate the phase morphology of polymer blends. Samples for SEM are easy to prepare and the morphology can be observed under high resolution [35].

Polymer blends have become a very important subject for scientific investigation in recent years because of their growing commercial acceptance. Copolymerization and blending are alternative routes for modification of properties of polymers. Blending is the least expensive method. It does not always provide a satisfactory alternative to copolymerization, of course, but polymer blends have been successfully used in an increasing number of applications in recent years. Such successes encourage more attempts to apply this technique to wider range of problems in polymer-related industries [30].

Polymer blends are important industrial materials with good properties to satisfy a wide range of applications. Mechanical properties of the blends, to a great extent, are

controlled by their morphology [36]. Kalkar et al. [37] postulated that PBT and PC can form one of the most successful commercial polymer blends. The PBT/PC blends have been commercialized under several trade names such as Xenoy®, Makroblend®/Pocan® and Ultrablend®. Impact modified PC/PBT blends have been used extensively in applications such as automotive bumpers where low temperature impact resistance and resistance to automotive fluids such as gasoline are required [38].

2.2 Compounding of PC/PBT in Twin Screw Extruders

Twin screw extruders have established a solid position in the polymer processing industry. The two main areas of application for twin screw extruders are profile extrusion of thermally sensitive materials and specialty polymer processing operations, such as compounding, devolatilization, chemical reactions, etc. Twin screw extruders used in profile extrusion have a closely fitting flight and channel profile and operate at restively low screw speeds, in the range of about 20 rpm. These machines offer several advantages over single screw extruder. Better feeding and more positive conveying characteristics allow the machine to process hard-to-feed materials (powders, slippery materials, etc.) and yield short residence times and a narrow residence time distribution (RTD). Better mixing and larger heat transfer area allow good control of the stock temperatures. Good control over residence times and stock temperatures obviously are key elements in the profile extrusion of thermally sensitive materials [39].

Twin screw extruders are generally classified by the direction of rotation: co-rotating and counter-rotating, and by the degree of intermeshing: non-intermeshing (tangential), completely or partially intermeshing. Currently, a wide variety of twin screw machines are being offered. Some find niches in specific applications, particularly when extensive devolatilization, high additive loadings, and/or intensive dispersive melt mixing are important [40].

The main distinction is made between intermeshing and non-intermeshing twin screw extruders. The latter are extruders where the flights of one screw do not protrude into the channel of the other screw. These extruders cannot form closed or semi-closed compartments and, therefore, do not have positive conveying characteristics. In intermeshing extruders, the degree of intermeshing can range from almost fully intermeshing to almost non-intermeshing with a corresponding range in the degree of positive conveying characteristics. However, it should be noted that fully intermeshing is a necessary, but not sufficient condition for positive conveying. In some geometrics, there is very little sealing of the screw channels, even when the screws are fully intermeshing. Positive conveying requires that the screw channels are closed off so that the material contained in the various channel sections is fully occluded. Any amount of back leakage into upstream channel sections will adversely affect the positive conveying behavior [41].

In intermeshing, co-rotating extruders, the materials are conveyed in a figure-eight pattern, alternating between moderate shear stress in the overflight zone (between screw and the barrel) and high shear stress in the apex zone. Owing to a segmented design, both the screw and the barrel can be custom-assembled to optimize for a specific production. The screw is usually made of several types of conveying and kneading mixing elements, both being able to convey the material either forward or backward. These extruders are easier to scale-up, provide good and adjustable balance between the dispersive and distributive mixing and they can be operated at restively high output rates [40].

The processes in the twin screw extruder depend primarily on the mode of operation (co- or counter-rotation) and degree of fill. The length of the feeding and melting zones can vary considerably, depending on the screw configuration and rotation speed, but in general these are much shorter in twin screw than for single screw machines. While in the single screw extruder, a continuous solid bed is formed, this does not happen in a twin

screw machine since the screw chambers are normally not totally filed and the solids conveying zone is continuously divided by intermeshing with the other screw [40].

The theory of twin screw extruders is not as well developed as the theory of single screw extruders. As a result, it is difficult to predict the performance of a twin extruder based on extruder geometry, polymer properties, and processing conditions. Conversely, it is equally difficult to predict the proper screw geometry when a certain performance is required in a particular application. This situation has led to twin screw extruders of modular design. These machines have removable screw and barrel elements. The screw design can be altered by changing the sequence of the screw elements along the shaft. In this way, an almost infinite number of screw geometries can be put together. The modular design, therefore, creates excellent flexibility and allows careful optimization of screw and barrel geometry of each particulars application. Unfortunately, modular screws and barrels also increase the cost of the extruder a great deal [39].

Experiments with two lab scale, intermeshing twin screw extruders were described by Rauwendall [41], one co- and one counter-rotating. Results are presented on power consumption, residence time distribution, and mixing characteristics of the two extruders. He postulated that the counter - rotating extruder exhibits a narrow residence time distribution and better dispersive mixing capability and the co-rotating extruder showed a better distributive mixing capability. He mentioned that the overall extruder performance seems to be dominated by the effect of the intermeshing region. He concluded that the co-rotating extruder appeared to be best suited for melt blending operations, while the counter-rotating extruder seems to be preferred in operations where solid fillers had to be dispersed in a polymer matrix.

Most of the information that has been published on co-rotating twin screw extruders has been the result of research and development studies conducted by machine manufactures

and a few of polymer producers. The isothermal flow of a Newtonian liquid in a co-rotating twin screw extruder having screw elements with three tips has been analyzed when the effect of the intermeshing zone on flow can be neglected. It was found that the values for four dimensionless parameters must be specified in order to obtain a unique relationship between the dimensionless axial pressure gradient and the dimensionless volumetric flow rate. These parameters included the number of screw tips, the helix angle, the ratio of the clearance to the screw radius, and the ratio of distance between screw centers to the radius [42].

Secor [43] postulated that twin-screw extruders are used very effectively, when partially filled, for mixing and surface renewal of high viscosity fluids. He suggested that the rate of energy input, often sufficiently high to be a major design consideration, determines the drive power, the heat input to the fluid, and the cooling requirements. A simple model for the rate of energy dissipation in twin-screw extruders predicts that the power input is proportional to the square of the screw speed. Meijer and Elemans [44] showed that a simplified model for a corotating twin-screw extruder is able to predict very well the correct energy consumption, specific energy, and temperature rise, not only over the extruder as whole, but also locally during processing (depending on local screw geometry, processing conditions, and material properties). They emphasized that this is of great practical importance in polymer processing because an understanding of the process is within reach and gives a perspective for solving problems in scale-up.

Gao et al. [45] presented and experimentally validated a physically motivated model for predicting the mean residence time in twin screw extruders. They showed that accurate estimation of the mean residence time and propagation delay through a plasticating extruder is critical for implementing feedback control schemes employing sensors mounted along the extruder. In their studies, experiments were carried out on a 30 mm Krupp Werner and Pfleiderer co-rotating twin screw extruder equipped with reflectance

optical probes over the melting section and mixing section and at the die. They demonstrated that the mean residence times predicted by their model are in good agreement with the experimentally measured ones. In their studies, both the model and experimental results indicate that the mean residence volume has a linear relationship with flow rate / screw speed ratio. They proposed that when the percent drag flow is not large, this model can be used to predict the mean residence time with an estimation error of no more than 10%. On the other hand, when the percent drag flow is large or higher estimation accuracy is required an improved mean residence time model can be used. They observed that operating conditions with equivalent specific throughput result in an equivalent residence-volume distribution (RVD) and residence-revolution distribution (RRD), and for a given screw configuration the axial mixing as measured by a tracer is essentially the same for all operating conditions. This allows the experimental RVD curves to be superimposed to form a single master curve for a given screw geometry. They identified that those new tools motivate the development of a simple residence model that characterizes the partially filled and fully filled screw sections and is capable of distinguishing between screw configurations and operating conditions.

Kumar et al. [46] developed a framework for improved operation of extruders in a wide range of applications by incorporating intelligent means for (i) on-line product quality estimation(inferential sensing), (ii) diagnostics for common process/material failures, and (iii) closed loop control of product quality based on the on-line estimation. In their study, they have developed a novel model-based approach for the estimation, diagnostics and controls in a unified framework.

Linjie and Xiaozheng [47] postulated that the melting of a polymer in co-rotating twin-screw extruders depends not only on screw configurations and operational conditions, but on the properties of the polymer as well. The progressive melting of polymer pellets in co-rotating twin-screw extrusion was so complicated and varying that it was nearly

impossible to be described and modeled by one single model. They suggested that it was modeled by selecting necessary melting sub-stages, so that the operating conditions and screw configuration could be optimized. Finally, Shah and Gupta [48] found that for similar screw cross-sections and rotational speed, the axial velocity as well as the degree of mixing is higher in the co-rotating extruder, whereas pressure builds up is higher in the counter-rotating extruder. In contrast to the flow in the co-rotating extruder, where the velocity was always maximum at the screw tips, in the counter rotating extruder the velocity was higher in the intermeshing zone. Since the counter-rotating twin-screw extruders, which are similar to gear pumps, provide the maximum positive displacement, they are the machine of choice for profile extrusion, whereas co-rotating twin-screw extruders are more suitable for other applications such as compounding, mixing, devolatization and chemical reaction. In this study, a co-rotating twin screw extruder was used for compounding of PC/PBT blends and details are explained in Chapter 3 of this thesis.

Chapter 3
EXPERIMENTAL

The experiments described in this chapter were all carried out on a WP ZSK 58 mm co-rotating extruder at the compounding facility of SABIC Innovative Plastics in Cobourg, Ontario. The resin used was a commercial Xenoy® PC/PBT blend and three sets of experiments were completed.

In these sets of experiments, the main objective was to evaluate the effects of processing conditions and resin composition on the rheological properties of the blend. For that purpose, a 2-level factorial design was employed with screw speed, and PC and PBT flow rates being the factors considered. The factorial design and experimental set up for these experiments are explained in section 3.1 and testing procedures for rheological property measurements are described in section 3.2.

3.1 Factorial Design of Experiments

A 2^3 factorial design provides the smallest number of runs for which 3 factors can be studied in a complete factorial design because there are only two levels for each factor. In this study, the three factors were screw speed, PC flow rate (feeder 1) and PBT flow rate (feeder 2), each at two levels. These levels were approximately 10 % from the nominal conditions which were used as the center point. The design was augmented with 5 replicate runs at the center point. This design was run on two consecutive days as shown in Tables 3.1 and 3.2. Due to machine operating limitations, some of the combinations of the levels were not feasible and were adjusted to practical levels of the factors studied. These amended combinations are specified with bold red color numbers in Tables 3.1and 3.2.

Table 3.1 : Factorial design of 1st set of experiments (die hole diameter = 4 mm)

Run Order	Screw Speed (N) (RPM)	Total Feed Rate (Q) (kg/hr)	Feeder PC (X_1)	Feeder PBT (X_2)
1	410	425	0.61	0.39
2	451	434	0.66	0.34
3	451	383	0.61	0.39
4	410	425	0.61	0.39
5	369	383	0.61	0.39
6	410	425	0.61	0.39
7	369	434	0.66	0.34
8	451	468	0.61	0.39
9	410	425	0.61	0.39
10	451	416	0.56	0.44
11	400 **(410)**	468	0.61	0.39
12	400 **(369)**	416	0.56	0.44
13	410	425	0.61	0.39

Table 3.2: Factorial design 2nd set of experiments (die hole diameter = 3 mm)

Run Order	Screw Speed (N) (RPM)	Feed Rate(Q) (kg/hr)	Feeder PC (X_1)	Feeder PBT (X_2)
1	410	425	0.61	0.39
2	451	434 **(456)**	0.66	0.34
3	451	383	0.61	0.39
4	410	425	0.61	0.39
5	369	383	0.61	0.39
6	410	425	0.61	0.39
7	369 **(390)**	434	0.66	0.34
8	451	468	0.61	0.39
9	410	425	0.61	0.39
10	451	416	0.56	0.44
11	400 **(451)**	468	0.61	0.39
12	400 **(369)**	416	0.56	0.44
13	410	425	0.61	0.39

A 3rd set of experiments was run as shown in Table 3.3. The screw speed, total feed rate, feed rate of PC (feeder 1) and feed rate of PBT (feeder 2) were kept constant for all nine runs in this set of experiments. The composition of the PC feeder was the only variable that was manipulated. These experiments were run randomly without any notice. In Table 3.3, Q is the total feed rate, N is the screw speed, Q_{PC} is the total feed of polycarbonate in feeder1, Q_{PBT} is the feed rate of poly (butylene terephthalate), X_{PC1} is the weight fraction of polycarbonate of type1 in feeder 1 and X_{PC2} is the weight fraction of polycarbonate type 2 in feeder 1. The experimental set up for this set of experiments was similar as those of 1st and 2nd set of experiments. The die used had 17 holes each with 3 mm diameter. For the total of 9 runs of experiments, 36 polymer samples were collected at intervals of 1, 5, 10, and 15 minutes for each run.

As indicated earlier, these experiments were carried out at the SABIC Innovative Plastics, Cobourg plant using a WP 58mm twin-screw extruder, with two feeders and a data acquisition system. The extruder was capable of running at a maximum screw speed of 620 rpm. The extruder was powered by a 250 HP drive, which provided a measurement of total screw load (estimated from motor current and voltage) and screw speed. The extruder had 9 thermocouples along the barrel length, 3 thermocouples along the die and heating elements to control the temperatures in the corresponding barrel zones. The signals for the machine variables were recorded using a data acquisition system. In these experiments the motor torque (or load), die pressure, feed-rates, screw speed, melt temperature were recorded at a sampling rate of 2 Hz. The die used on the first day had 17 holes each with 4 mm diameter and the die used on the second day had 17 holes but each with 3 mm diameter. The material used was again a Xenoy ® blend. Polymer samples were collected during each run. A total of 143 samples were collected on the first day at intervals of 0.5 , 1 , 1.5 , 2 , 2.5 , 3 , 3.5 , 4 , 9 , 14 and 19 minutes for each run. On the second day, totally 156 samples were collected at intervals of 0.5 , 1 , 1.5 , 2 , 2.5 , 3 , 3.5 , 4 , 6 , 8 ,10 and 15 minutes for each run.

Table 3.3 : 3rd set of experiments

Run Number	Q Total feed rate (kg/hr)	N Screw speed (rpm)	Q_{PC} (kg/hr) Feeder1	Q_{PBT} (kg/hr) Feeder2	X_{PC} in Feeder1	X_{PBT} in Feeder2	X_{PC1} in Feeder1	X_{PC2} in Feeder1
1	425	410	259.25	165.75	0.61	0.39	0.428	0.389
2	425	410	259.25	165.75	0.61	0.39	0.428	0.389
3	425	410	259.25	165.75	0.61	0.39	0.478	0.339
4	425	410	259.25	165.75	0.61	0.39	0.378	0.439
5	425	410	259.25	165.75	0.61	0.39	0.428	0.389
6	425	410	259.25	165.75	0.61	0.39	0.428	0.389
7	425	410	259.25	165.75	0.61	0.39	0.328	0.489
8	425	410	259.25	165.75	0.61	0.39	0.528	0.289
9	425	410	259.25	165.75	0.61	0.39	0.428	0.389

3.2 Testing Procedures

3.2.1 Melt Volume-Flow Rate (MVR)

Melt Volume-Flow Rate (MVR) or Melt Flow Index (MFI) is the most common quality index which characterizes the flow behavior of polymer melts with a single number (single-point measurement). The melt flow indexer is normally located in the laboratory and not directly at the production line; hence the MFI value is determined 'off-line' [49].

The major method used in the plastics industry today is the Melt Flow Rate Test (MFR), sometimes referred to as the Melt Flow Index (MFI). Although the limitations of this test have been known and discussed for many years, it is widely used and standard test procedures have been established for most polymers (ASTM D1238-95 or ISO 1133).

The almost universal acceptance of this test has arisen from the fact that it gives an indication of quality while being simple, easy to operate, fast and, most importantly, inexpensive. These single point data are plotted versus time on control charts to establish the variability of the process and the consequential product quality [50].

The Melt Flow Index test originated in the laboratories of ICI and was specified as a standard rheological quality control test in the ISO, BS, and ASTM. Despite the fact that MFI is an empirically defined parameter with certain limitations, it is still one of the most popular parameters in the plastics industry for distinguishing various grades of polymers. Polymer manufacturers have used it routinely to specify the most suitable end use of a particular grade of the polymer [51]. The melt flow index is related to the inverse of viscosity; however, no end-loss corrections have been developed. The molten polymer in the reservoir is extruded through a capillary by the force weights which load a piston.

According to the measuring procedure and the dimensions of the reservoir, the piston and the capillary are standardized worldwide [49].

By ASTM standards, melt flow index (MFI) is defined as the number of grams of polymer that can be pushed out of a capillary die of standard dimensions (diameter: 2.095 mm, length: 8.0 mm) under the action of standard weight (2.16 kg for PE, at 190°C) in 10 minutes (ASTM Standard 1238). In this study, in all three sets of experiments MVR values were measured in the SABIC Innovative Plastics industry's laboratory and followed their own standard. The amount of polymer that came out through the die after a specific interval was weighed and normalized to the number of grams that would have been extruded in 10 minutes. It is noted that the test results are reported by melt volume flow rate (MVR), which is melt flow index (MFI) divided by polymer melt density i. e. , MVR (cm^3/10 min) = MFI (g/10 min) / ρ (g/cm^3) .

3.2.2 Parallel Plate Rheometer

In a parallel plate rheometer, one plate rotates whilst the other is stationary, and the torque and normal force are measured. The sample volume is not as strong a function of the plate's radius as for the cone-and-plate geometry. The shear rate in this geometry is a function of the radius measured from the centre. Dynamic shear properties, such as storage and loss moduli are measured when one plate oscillates relative to other. When small gaps are used, one must take into account the small yet finite movement of the non-oscillating plate, even when a force rebalances torque head is used [49]. It is easier to load and unload viscous or soft solid samples with parallel plate geometry than with one and plate or concentric cylinders. Thus parallel plates are usually preferred for measuring viscoelastic material functions [52].

Dynamic rheological measurements for storage modulus G' and loss modulus G" were made on a parallel plate rheometer (AR2000, TA Instruments) with 25 mm diameter parallel plates and a 900nm gap set. Samples were dried at 120^0C in a vacuum oven for two hours. The sample were prepared as disks (Diameter=25mm, Thickness=1 mm) using hot press at 260^0C. Liquid nitrogen run through to pressurize the oven in order to provide a nonreactive atmosphere during the experiment. The measurements were carried out at 270^0C and dynamic frequency sweeps were made over range of 0.01 – 100 Hz for 1^{st} and 2^{nd} set of experiments, and 1-100 Hz for 3^{rd} set of experiments. Details results are discussed in chapter 4.2.

3.2.3 Capillary Rheometer

The simplest and most ubiquitous type of melt rheometer is the capillary rheometer. While it is not very versatile in its capabilities, its popularity makes it important for the practitioner to understand its proper use and limitations. Capillary rheometers are used primarily to determine the viscosity in the shear rate range of 5 to 1000 s^{-1}, although very long capillaries have occasionally been used to extend the range to much lower shear rates [32].

The capillary rheometer, however, has many of the elements required to simulate the operation of the machines used in polymer processing. It is similar to the MFR instrument, with a temperature-controlled barrel containing a piston that forces molten polymer through a capillary die of fixed dimensions. In the capillary rheometer, however, extrusion of the polymer is driven by a motor and screw or servo-hydraulic system. A load cell on the piston or a pressure transducer in the rheometer barrel measures the extrusion forces. The force necessary to produce flow (shear stress) and the rate of flow (shear rate) are then used to calculate the viscosity or resistance to flow:

Viscosity, (η) = Shear Stress/Shear Rate

This rheometer is able to reproduce the deformation rates and forces at which polymer is actually processed (many of the early extruders and injection molding machines used a ram instead of a screw) and thus can simulate the conditions seen in a conversion process [50].

Capillary viscosity measurements were made by a Galaxy V Capillary Rheometer (Model 8052; Kayeness Inc. : A Dynisco Company). The capillary size was 0.03 inch in diameter and 1.2 inch in length (L/D = 40). The samples were dried in a vacuum oven at temperature 120^0C for two hours. The dry sample was charged into the heated barrel of the capillary rheometer which was set at 270^0C. Test was started after a 5 minute soak time.

3.2.4 Scanning Electron Microscopy (SEM)

According to literature reports, particle characterization can be achieved using electron spectroscopy for chemical analysis (ESCA), photon correlation spectroscopy (PCS), X-ray diffraction, transmission electron microscopy (TEM), scanning electron microscopy (SEM), and various other physical methods. Among all the techniques, SEM is the easiest visual technique to obtain information about the average size, size distribution, and the surface morphology of particles [53].

In the conventional scanning electron microscope (SEM), image contrast can be produced either by variations in sample topography or by differences in chemical composition. Secondary electron images, which are most commonly used in SEM analyses, are generally dominated by topographical features and only weakly modulated by variations in substrate composition. Although more sensitive to compositional variations,

corresponding backscattered images have been of less interest because of their poorer quality and resolution. These deficiencies have only recently been overcome with improved detection systems. Chemical contrast differences provide a viable and useful means of characterizing multiphase polymer systems by scanning electron microscopy [54].

Scanning Electron Microscopy (SEM) is a popular technique for assessing the structure in a polymer blend. This method focuses an electron beam onto a surface, and the emission of electrons from specimen is detected and amplified to obtain a image. The resultant image is often viewed on a video monitor. SEM exhibits a relatively large depth of fields, thus can show topological features better than other microscopy methods (except perhaps atomic force microscopy). Staining and etching processes can be employed to provide improved contrast. SEM is particularly useful for the observation of fracture surfaces [55]. Ruthenium tetraoxide (RuO_4) is a powerful oxidizing agent and readily attacks a *variety* of functional groups and aromatic systems. Ruthenium would appear to offer several practical advantages in that it is less volatile, less toxic, less expensive, and more readily available than osmium [56].

The morphologies of the fractured surfaces of the blends were observed in a scanning electron microscope (FESEM 1530, with EDX Pegasus 1200 integrated). The blend specimens were cryo-fractured in liquid nitrogen to produce brittle surfaces, which were then stained by RuO_4 vapour. Ruthenium tetraoxide was obtained by reacting $RuCl_3$ with excess amount of $NaIO_4$. RuO_4 staining was employed in order to reveal more detail information on the morphology at a better contrast under a SEM microscope. They were then coated with a thin layer of gold prior to SEM observations. Both secondary electron (SE) detector and reel backscattering electron (RBSE) detector were used in this study. Three time durations were used for staining the samples. Those were: a) overnight

(around 14 hrs), b) 2 hrs, and c) 1 hr. Unstained samples were also prepared for comparisons.

In this study, three different types of samples were used for SEM tests. Those were:

a) PC/PBT blend pellets,
b) PC/PBT blend sample, but collected after completing the rheological test in the parallel plate rheometer, and
c) PC/PBT blend sample, but collected after completing the rheological test in the capillary rheometer

These samples were obtained from the 2nd set experiments, run number 13 at a 10 minute time interval.

Chapter 4

RESULTS AND DISCUSSION

PC/PBT blends were characterized in this study. Melt volume-flow rate (MVR) data were measured by using an extrusion plastomer, rheological properties were obtained by using parallel plate and capillary rheometers, and finally the morphology of PC/PBT blends was observed by scanning electron microscopy (SEM). The results of melt volume-flow rate for all of three set of experiments are presented in section 4.1 of this chapter. In sections 4.2 and 4.3, the rheological properties of PC/PBT blends are discussed along with the Cox-Merz rule validity. The morphology of PC/PBT blend pellets and samples collected after testing in both parallel plate and capillary rheometers is finally discussed in section 4.4 of this chapter.

4.1 Melt Volume-Flow Rate (MVR)

Polymer samples were collected as a function of time during all three sets of experiments. The method for MVR measurements was described in chapter 3. All the MVR measurements were carried out on an extrusion plastomer at SABIC Innovative Plastics plant in Cobourg, ON. Each MVR measurement took around 20 minutes and results are shown in Tables 4.1.1, 4.1.2 and 4.1.3.

Table 4.1.1 : Melt Volume Rate (MVR) measurement results for 1st set of experiments (where N stands for the screw speed, Q for the volumetric flow rate, X_1 for the weight fraction of PC and X_2 for the weight fraction of PBT).

Run No.	N (rpm)	Q (kg/ hr)	X_1 (PC)	X_2 (PBT)	Instantaneous Melt Volume Rate(MVR) measurements										
					Sampling time(minute)										
					0.5	1	1.5	2	2.5	3	3.5	4	9	14	19
1	410	425	0.61	0.39	15.4	14.2	15.8	14.8	18.7	17.2	17.4	16.8	16.8	17.2	17.2
2	451	434	0.66	0.34	16.9	16.7	13.8	15.4	15.6	14.9	15.6	15.6	15.0	*--	12.4
3	451	383	0.61	0.39	18.2	19.5	17.9	18.9	18.6	18.8	19.4	19.1	20.0	20.9	20.7
4	410	425	0.61	0.39	17.2	16.4	16.3	16.1	15.8	16.2	16.6	16.3	15.8	15.7	16.3
5	369	383	0.61	0.39	16.5	16.7	17.0	15.9	16.4	16.1	16.1	16.1	16.3	17.5	16.3
6	410	425	0.61	0.39	16.8	16.4	16.2	16.8	15.4	16.0	15.6	15.4	18.2	18.5	17.2
7	369	434	0.66	0.34	15.9	15.9	16.5	16.0	15.0	14.7	15.0	14.5	13.3	13.4	13.2
8	451	468	0.61	0.39	17.8	18.1	16.8	16.3	17.1	17.0	16.5	16.4	16.8	15.7	17.6
9	410	425	0.61	0.39	14.5	15.4	15.2	15.8	15.8	16.2	13.9	16.3	17.4	16.8	17.1
10	451	416	0.56	0.44	20.6	21.3	21.6	20.7	21.0	20.6	21.8	22.4	21.0	20.3	21.4
11	410	468	0.61	0.39	15.3	15.7	16.6	16.3	19.8	16.4	15.6	15.2	15.2	--	--
12	369	416	0.56	0.44	16.9	16.0	16.6	16.4	16.9	16.9	17.3	17.2	17.4	--	--
13	410	425	0.61	0.39	16.8	17.2	16.8	17.1	17.6	17.8	18.3	17.4	17.4	18.0	17.7

* Missing sample indicated by --

Table 4.1.2: Melt Volume Rate (MVR) measurement results for 2nd set of experiments (where N is the screw speed, Q is the volumetric flow rate, X_1 is the weight fraction of PC and X_2 is the weight fraction of PBT).

Run No.	N (rpm)	Q (kg/ hr)	X_1 (PC)	X_2 (PBT)	Instantaneous Melt Volume Rate(MVR) measurements											
					Sampling time(minute)											
					0.5	1.0	1.5	2.0	2.5	3.0	3.5	4.0	6.0	8.0	10	15
1	410	425	0.61	0.39	16.2	17.7	18.7	18.2	18.7	20.5	19.4	18.0	16.8	18.5	15.3	18.6
2	451	456	0.66	0.34	17.4	15.6	18.4	17.0	19.9	20.1	19.0	19.0	20.4	19.3	20.7	19.5
3	451	383	0.61	0.39	21.7	23.0	23.4	26.3	26.0	25.5	24.5	25.0	24.8	24.3	25.4	23.8
4	410	425	0.61	0.39	18.5	19.1	19.0	18.7	18.6	18.8	18.8	19.1	19.2	19.3	20.1	19.2
5	369	383	0.61	0.39	17.9	19.5	18.9	19.0	18.7	18.8	19.1	20.0	18.2	19.2	19.5	17.9
6	410	425	0.61	0.39	16.7	18.2	19.0	18.8	19.3	19.8	18.6	18.9	19.3	19.1	19.4	19.8
7	390	434	0.66	0.34	17.9	16.9	16.5	18.6	17.5	17.5	17.5	16.2	16.9	17.4	16.4	17.3
8	451	468	0.61	0.39	20.5	20.5	20.4	20.6	20.9	20.1	20.3	20.5	20.9	20.4	21.0	20.1
9	410	425	0.61	0.39	19.2	19.3	19.6	18.6	19.4	20.3	19.3	20.5	20.2	20.7	21.2	20.3
10	451	416	0.56	0.44	25.8	25.0	25.3	25.0	25.0	24.9	25.9	25.0	25.9	24.0	25.7	26.4
11	451	468	0.61	0.39	19.5	20.5	20.6	21.0	20.9	20.9	20.0	23.0	19.8	20.0	20.5	20.4
12	369	416	0.56	0.44	20.5	20.2	20.3	19.8	20.4	20.1	21.5	20.8	19.7	19.6	19.5	20.5
13	410	425	0.61	0.39	18.3	19.6	20.0	20.0	20.1	20.3	20.9	20.6	21.1	21.0	20.2	20.8

Table 4.1.3 : Melt Volume Rate (MVR) measurement results for 3rd set of experiments (where Q is the total flow rate, N is screw speed, Q_{PC} is the total flow rate of PC, Q_{PBT} is flow rate of PBT, F1 means feeder1, and F2 means feeder2).

Run No.	Q (kg/hr)	N (rpm)	Q_{PC} (kg/hr) F1	Q_{PBT} (kg/hr) F2	X_{PC} in F1	X_{PBT} in F2	X_{PC1} in F1	X_{PC2} in F1	Instantaneous Melt Volume -Flow Rate (MVR) measurements			
									Sampling time(minute)			
									1.0	5.0	10	15
1	425	410	259.25	165.75	0.61	0.39	0.428	0.389	19.2	20.3	19.6	20.5
2	425	410	259.25	165.75	0.61	0.39	0.428	0.389	19.2	21.7	20.6	20.0
3	425	410	259.25	165.75	0.61	0.39	0.478	0.339	18.9	19.2	19.4	19.4
4	425	410	259.25	165.75	0.61	0.39	0.378	0.439	18.6	18.4	19.0	18.6
5	425	410	259.25	165.75	0.61	0.39	0.428	0.389	20.6	18.8	18.6	18.9
6	425	410	259.25	165.75	0.61	0.39	0.428	0.389	21.1	19.6	18.9	19.2
7	425	410	259.25	165.75	0.61	0.39	0.328	0.489	20.1	19.3	18.8	18.9
8	425	410	259.25	165.75	0.61	0.39	0.528	0.289	18.1	18.4	17.6	18.0
9	425	410	259.25	165.75	0.61	0.39	0.428	0.389	20.9	20.3	21.3	20.9

In order to assess the measurement error, some melt volume-flow rate (MVR) measurements were randomly repeated under identical conditions. Results of the replicated measurements with the average value are shown in Tables 4.1.4, 4.1.5 and 4.1.6.

Table 4.1.4 : Replicate MVR measurements for 1st set of experiments

Run No.	Sampling time (min)	MVR Measurement	Replicate MVR Measurement	Average
1	19	17.2	17.3	17.3
5	19	16.3	16.6	16.5
10	19	21.4	22.5	22.0
13	19	17.7	17.7	17.7

Table 4.1.5. : Replicate MVR measurements for 2nd set of experiments

Run No.	Sampling time (min)	MVR Measurement	Replicate MVR Measurement	Average
1	10	15.3	14.2	14.8
2	10	20.7	19.7	20.2
3	10	25.4	24.5	25.0
4	10	20.1	20.2	20.2
5	10	19.5	20	19.8
6	10	19.4	19.3	19.4
7	10	16.4	16.6	16.5
8	10	21	20.8	20.9
9	10	21.2	20.5	20.9
10	10	25.7	25.9	25.8
11	10	20.5	20.7	20.6
12	10	19.5	19.3	19.4
13	10	20.2	19.9	20.1

Table 4.1.6 : Replicate MVR measurements for 3rd set of experiments

Run No.	Sampling time (min)	MVR Measurement	Replicate MVR Measurement	Average
3	15	19.4	19.2	19.3
7	15	18.9	19.3	19.1
8	15	18	17.9	18.0
9	15	20.9	20.6	20.8

Inspection of the data in Tables 4.1.4, 4.1.5 and 4.1.6 shows the measurement reproducibility is quite good and therefore the error is small.

In extrusion, the total shear the polymer experiences is related to the shear rate and mean residence time. Shear rate and residence time depend on screw speed and polymer feed rate. Generally, when the feed rate increases, the average residence time decreases. When the screw speed increases, the shear rate increases. The variation profiles of MVR with changing feed rates of PC and PBT, and also changing the screw speed are now discussed.

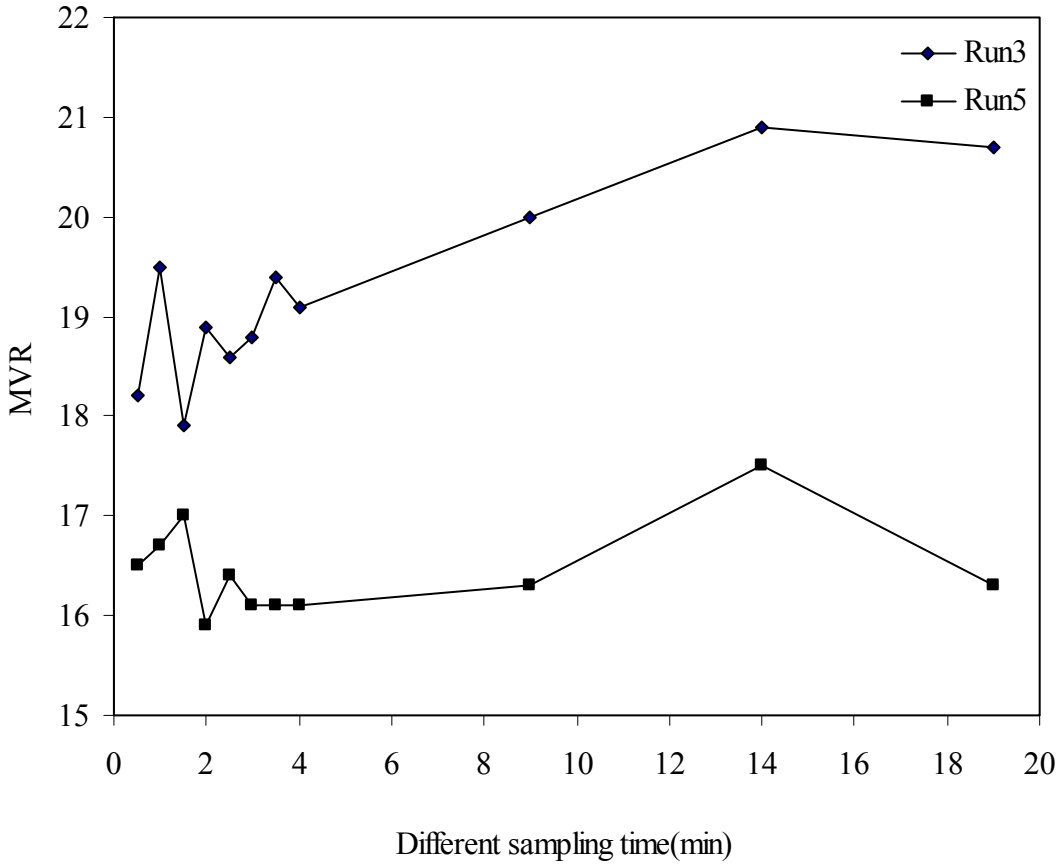

Fig. 4.1.1: Variation of Melt Volume-Flow Rate (MVR) with sampling time for Run 3 and Run 5 of 1st set of experiments.

Fig 4.1.1 compares the MVR measurements for the two runs from the 1st set of experiments. Run3 and Run5 have the same feed-rate (383 kg/hr), but different screw-speeds (451 and 369 rpm respectively). The average MVRs of Run3 and Run5 are 19.3 and 16.4, respectively. Fig. 4.1.1 shows that higher screw speed results in higher MVR value at constant feed rate. Similar behaviour is observed in Fig. 4.1.2 for runs 10 and 12 of the 2nd set of experiments.

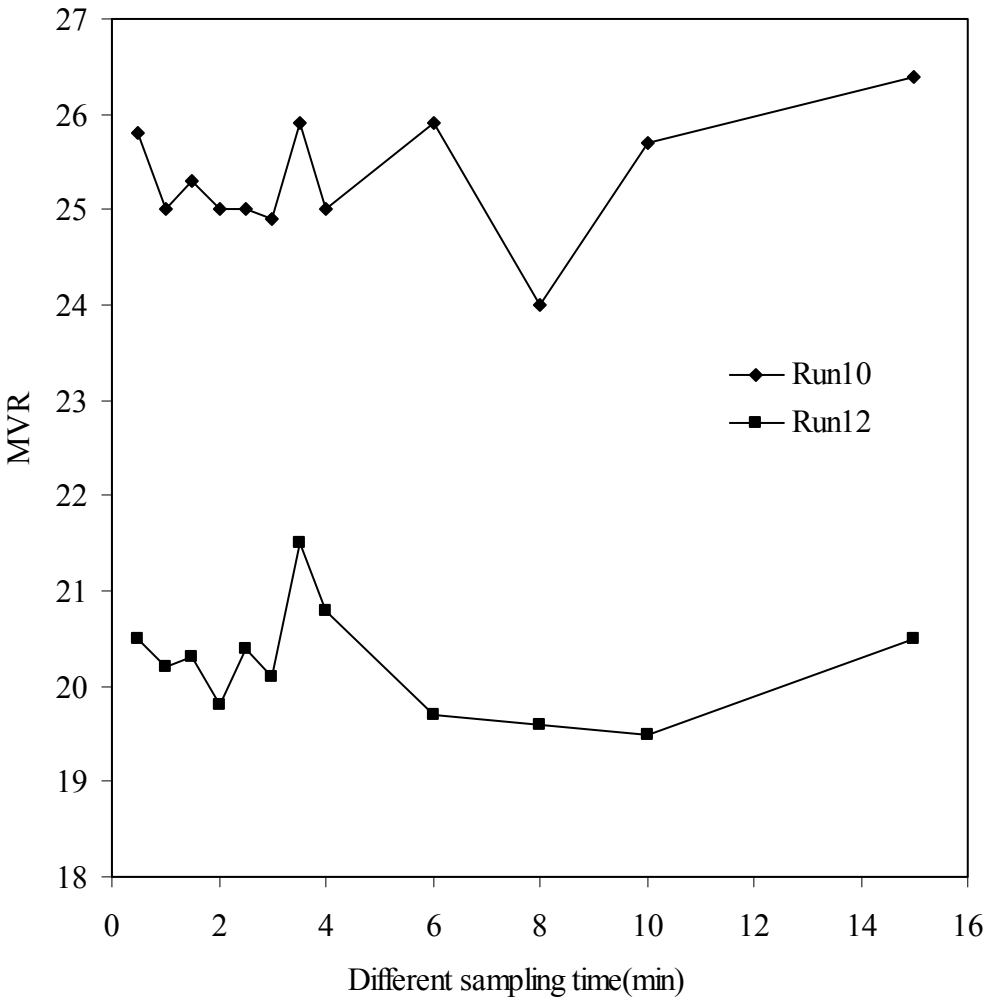

Fig. 4.1.2: Variation of Melt Volume-Flow Rate (MVR) with sampling time for Run 10 and Run 12 of 2nd set of experiments.

Run10 and Run12 have the same feed-rate (416 kg/hr), but different screw-speeds (451 and 369 rpm, respectively). The higher screw-speed again results in higher MVR. The average MVRs of Run10 and Run12 are 25.3 and 20.2, respectively.

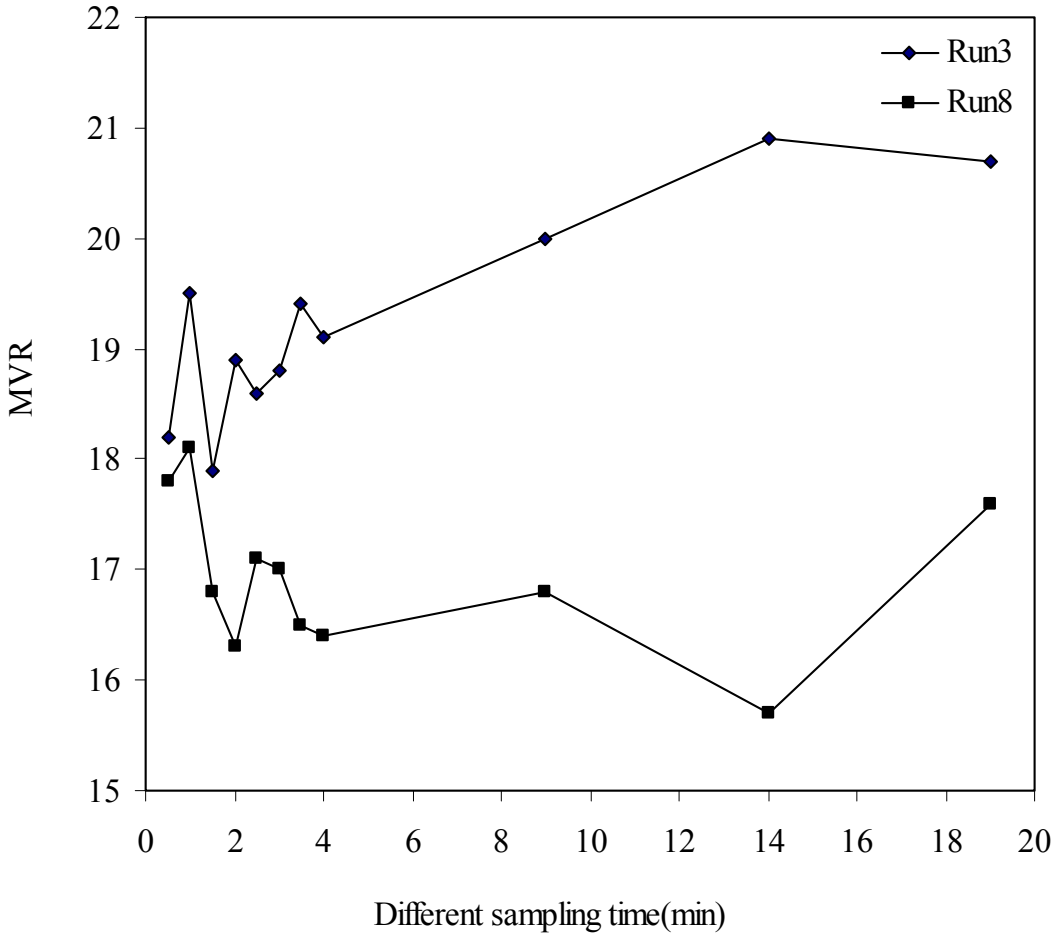

Fig. 4.1.3: Variation of Melt Volume-Flow Rate (MVR) with sampling time for Run 8 and Run 5 of 1st set of experiments.

The effect of feed rate at constant screw speed is highlighted in Fig 4.1.3. Run 3 and Run 8 have the same screw-speed (451 rpm), but different feed-rates (383 and 468 kg/hr, respectively). Increased flow rate results in lower residence time that leads to reduced MVR. The average MVR of Run 3 and Run 8 are 19.3 and 16.9, respectively. The same trends are shown in Fig. 4.1.4. In this figure, Run 5 and Run 12 have the same

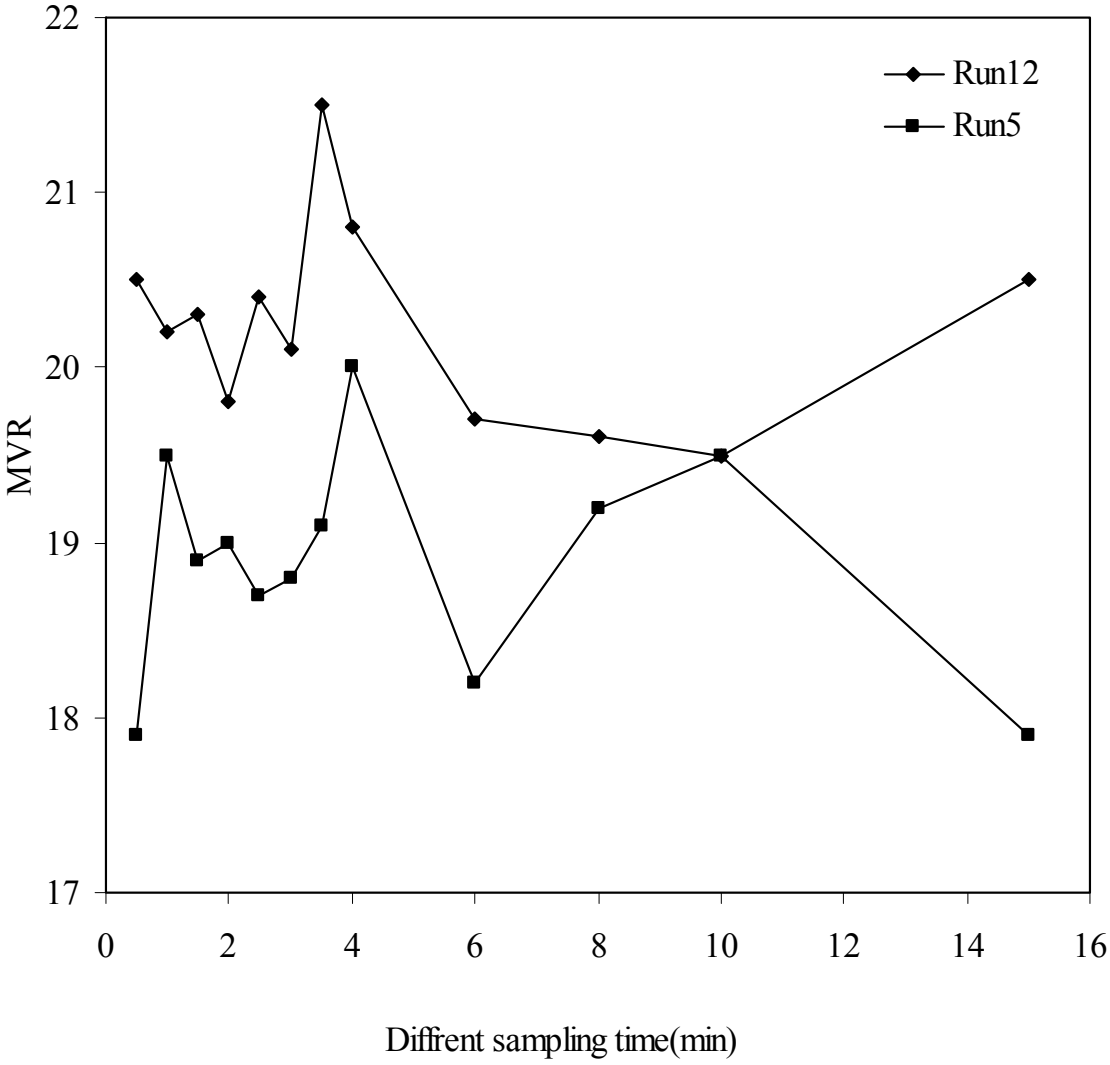

Fig. 4.1.4: Variation of Melt Volume-Flow Rate (MVR) with sampling time for Run 8 and Run 5 of 2nd set of experiments.

screw-speed (369 rpm), but different feed-rate (383 and 416 kg/hr, respectively). The average MVR of Run5 and Run12 are 18.9 and 20.2 respectively.

For all the centre points runs (i.e., run numbers 1, 4, 6, 9 and 13) of 1st and 2nd set of experiments screw speed, feed rate and composition of PC and PBT are the same. Tables 4.1.7 and 4.1.8 show average MVR values for the 1st and 2nd set of experiments, respectively. In these experiments, the screw speed, feed rate and composition of PC were 410 rpm, 425 kg/hr and 0.61, respectively. Figures 4.1.5 and 4.1.6 show variations of MVR with sampling times for the centre points runs. Although all the runs had the same variable levels, these figures show different MVR. This difference in MVR can be attributed to different levels of degradation due to different dies used in these experiments [57]. The die used in the second set of experiments was more restrictive resulting in higher degree of fill in the extruder, thus leading to more shearing and degradation. Finally, the MVR measurements show that the time interval from 0 to 5 minutes is transient.

Table 4.1.7: Average MVR of Run 1, 4, 6, 9 and 13 of 1st set of experiments

Run No.	Average MVR
1	16.5
4	16.2
6	16.6
9	15.9
13	17.4

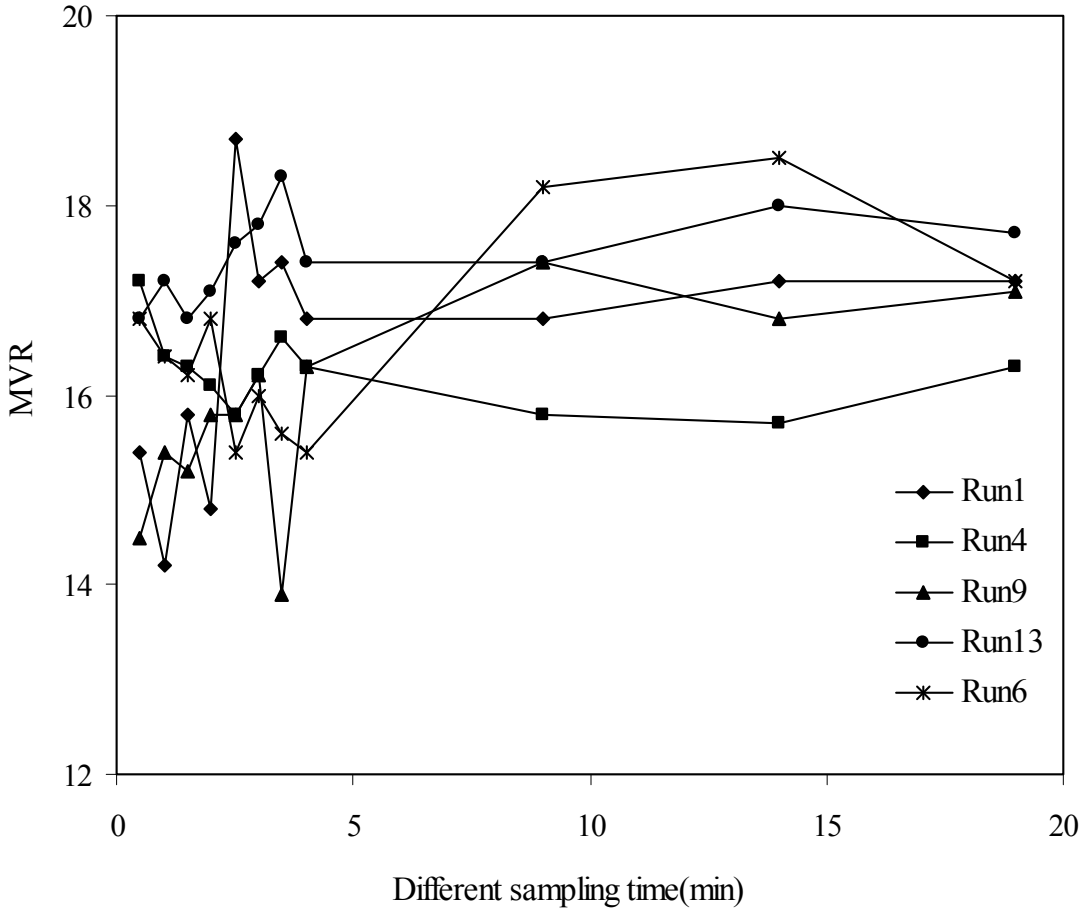

Fig. 4.1.5: Variation of Melt Volume-Flow Rate (MVR) with sampling time for Runs 1, 4, 6, 9 and 13 (centre points) of 1st set of experiments

Table 4.1.8: Average MVR of Run 1, 4, 6, 9 and 13 of 2nd set of experiments

Run No.	Average
1	18.1
4	19.0
6	18.9
9	19.9
13	20.2

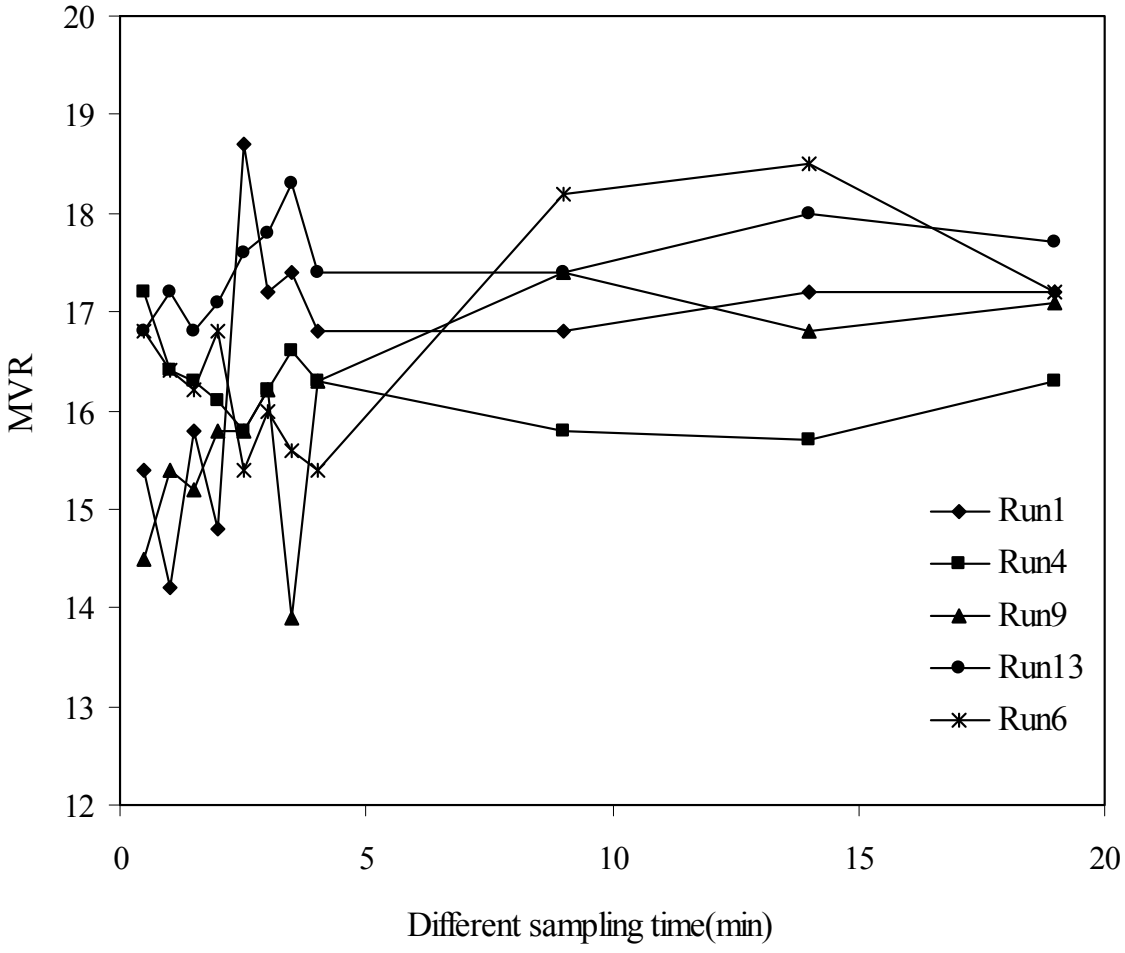

Fig. 4.1.6: Variation of Melt Volume-Flow Rate (MVR) with sampling time of Runs 1, 4, 6, 9 and 13 (centre points) of 2nd set of experiments

4.1.1 Statistical Analysis

Analysis of variance (ANOVA) of the 1st and 2nd set of experiments was done in this section. It was already mentioned in section 3.1 that both of these set of experiments were conducted using 2^3 factorial design of experiments and due to machine operating limitations, some of the combinations of the levels were not feasible and were adjusted to practical levels of the factors studied. These amended combinations are specified with bold red color numbers in Tables 3.1 and 3.2 in Chapter 3.

4.1.1.1 Variance Analysis

Table 4.1.9: Analysis of variance (ANOVA) for 1st set of experiments

Factor	ANOVA; Var.:MVR; R-sqr=.92288 3 factors, 1 Blocks, 13 Runs; MS Residual=.4354181				
	SS	df	MS	F	p-value
N(rpm)	8.71360	1	8.71360	20.01203	0.00422
Q_{PC}(kg/hr)	13.19721	1	13.19721	30.30928	0.00150
Q_{PBT}(kg/hr)	3.26684	1	3.26684	7.50276	0.033775
N by Q_{PC} Interaction	4.85132	1	4.85132	11.14175	0.01565
N by Q_{PBT} Interaction	0.39655	1	0.39655	0.91073	0.37677
Q_{PC} by Q_{PBT} Interaction	0.02901	1	0.02901	0.06662	0.80494
Error	2.61251	6	0.43542		
Total SS	33.87692	12			

Where, SS = Sum of squares, df = Degrees of freedom, MS = Mean squares, F = Variance ratio, p = Probability

Table 4.1.9 shows that the melt volume-flow rate (MVR) of 1st of experiments is significantly affected by the screw speed (N), flow rate of PC (Q_{PC}) and PBT (Q_{PBT}), and interaction between screw speed (N) and flow rate of PC (Q_{PC}).

Table 4.1.10: Analysis of variance (ANOVA) for 2nd set of experiments

Factor	ANOVA; Var.:MVR; R-sqr=.92288 3 factors, 1 Blocks, 13 Runs; MS Residual=.4354181				
	SS	df	MS	F	p-value
N(rpm)	20.08822	1	20.08822	21.25202	0.00365
Q_{PC}(kg/hr)	20.87503	1	20.87503	22.08441	0.00332
Q_{PBT}(kg/hr)	0.00167	1	0.00167	0.00177	0.96780
N by Q_{PC} Interaction	0.01039	1	0.01039	0.01099	0.91993
N by Q_{PBT} Interaction	0.16812	1	0.16812	0.17786	0.68790
Q_{PC} by Q_{PBT} Interaction	0.76881	1	0.76881	0.81335	0.40188
Error	5.67143	6	0.94524		
Total SS	64.74769	12			

Table 4.1.10 shows that the melt volume-flow rate (MVR) of 2nd set of experiments is significantly affected by the main factors being screw speed (N) and flow rate of PC (Q_{PC}), and interaction between flow rate of PC(Q_{PC}) and PBT (Q_{PBT}).

4.1.1.2 Effect of Different Factors by Variance Analysis

Table 4.1.11: Effect Estimations by analysis of variance (ANOVA) for 1st set of experiments

Factor	Effect Estimates; Var.:MVR; R-sqr=.92288; 3 factors, 1 Blocks, 13 Runs; MS Residual=.4354181									
	Effect	Std. Err.	t(6)	p-value	-95.% Cnf.Limt	+95.% Cnf.Limt	Coeff	Std.Err. Coeff.	-95.% Cnf.Limt	+95.% Cnf.Limt
Mean/ Interc.	16.89	0.18	92.21	0.000	16.44	17.34	16.89	0.18	16.44	17.34
N(rpm)	2.09	0.47	4.47	0.004	0.95	3.23	1.04	0.23	0.47	1.61
Q_{PC} (kg /hr)	-2.53	0.46	-5.51	0.002	-3.66	-1.41	-1.27	0.23	-1.83	-0.70
Q_{PBT} (kg/hr)	1.24	0.45	2.74	0.034	0.13	2.34	0.62	0.23	0.07	1.17
N by Q_{PC} Interaction	-1.54	0.46	-3.34	0.016	-2.66	-0.41	-0.77	0.23	-1.33	-0.20
N by Q_{PBT} Interaction	0.43	0.45	0.95	0.377	-0.67	1.53	0.22	0.23	-0.34	0.77
Q_{PC} by Q_{PBT} Interaction	0.11	0.44	0.26	0.805	-0.97	1.20	0.06	0.22	-0.49	0.60

From Table 4.1.11**,** ANOVA describes the relation between MVR and main factors and interaction effect for the 1st set of experiments as follows:

$$MVR = 16.89 + 2.09 \times N - 2.53 \times Q_{PC} + 1.24 \times Q_{PBT} - 1.54 \times N \times Q_{PC}$$

The above equation shows that MVR increases with increasing N and Q_{PBT}, and reverses with the value of Q_{PC} and interaction of N × Q_{PC}**.** This is expected since: (i) increasing N increases shear rate and may lead to increased degradation that results in reduced viscosity and therefore increased

MVR, (ii) PC is the high molecular weight component, so increasing its flow rate will decrease MVR and (iii) PBT is the low molecular weight component, so increasing its flow rate will increase MVR. This agrees with the results of Figs. 4.1.1 and 4.1.2 where the MVR increases as screw speed increases.

Table 4.1.12 Effect Estimations by analysis of variance (ANOVA) for 2nd set of experiments

Factor	Effect Estimates; Var.:MVR; R-sqr=.92288; 3 factors, 1 Blocks, 13 Runs; MS Residual=.4354181									
	Effect	Std. Err.	t(6)	p-value	-95.% Cnf.Limt	+95.% Cnf.Limt	Coeff	Std.Err. Coeff.	-95.% Cnf.Limt	+95.% Cnf.Limt
Mean/ Interc.	19.05	0.41	47.02	0.000	18.05	20.04	19.05	0.41	18.05	20.04
N(rpm)	5.49	1.19	4.61	0.004	2.58	8.41	2.75	0.60	1.29	4.20
Q_{PC} (kg /hr)	-5.77	1.23	-4.70	0.003	-8.78	-2.77	-2.89	0.61	-4.39	-1.38
Q_{PBT} (kg/hr)	0.04	1.04	0.04	0.967	-2.51	2.60	0.02	0.52	-1.25	1.30
N by Q_{PC} Interaction	0.13	1.24	0.10	0.920	-2.91	3.17	0.07	0.62	-1.46	1.59
N by Q_{PBT} Interaction	0.40	0.95	0.42	0.688	-1.93	2.74	0.20	0.48	-0.97	1.37
Q_{PC} by Q_{PBT} Interaction	-1.02	1.13	-0.90	0.401	-3.78	1.74	-0.51	0.56	-1.89	0.87

From Table 4.1.12, ANOVA describes the relation between MVR and main factors and interaction effect for the 2nd set of experiments as follows:

$$MVR = 19.05 + 5.49 \times N - 5.77 \times Q_{PC} - 1.02 \times Q_{PC} \times Q_{PBT}$$

It shows that the melt volume-flow rate (MVR) is significantly affected by screw speed (N), flow rate of PC(Q_{PC}); and interaction of PC(Q_{PC}) and PBT(Q_{PBT}).

4.1.1.3 Comparison of Predicted and Observed Values

For the 1st set of experiments, variations of predicted values with observed values are shown in Fig. 4.1.7. It is demonstrated that a linear relationship exists between predicted and observed values of MVR, and five centre points are parallel to X-axis. Same behavior for the 2nd set of experiments is shown in Fig.4.1.8.

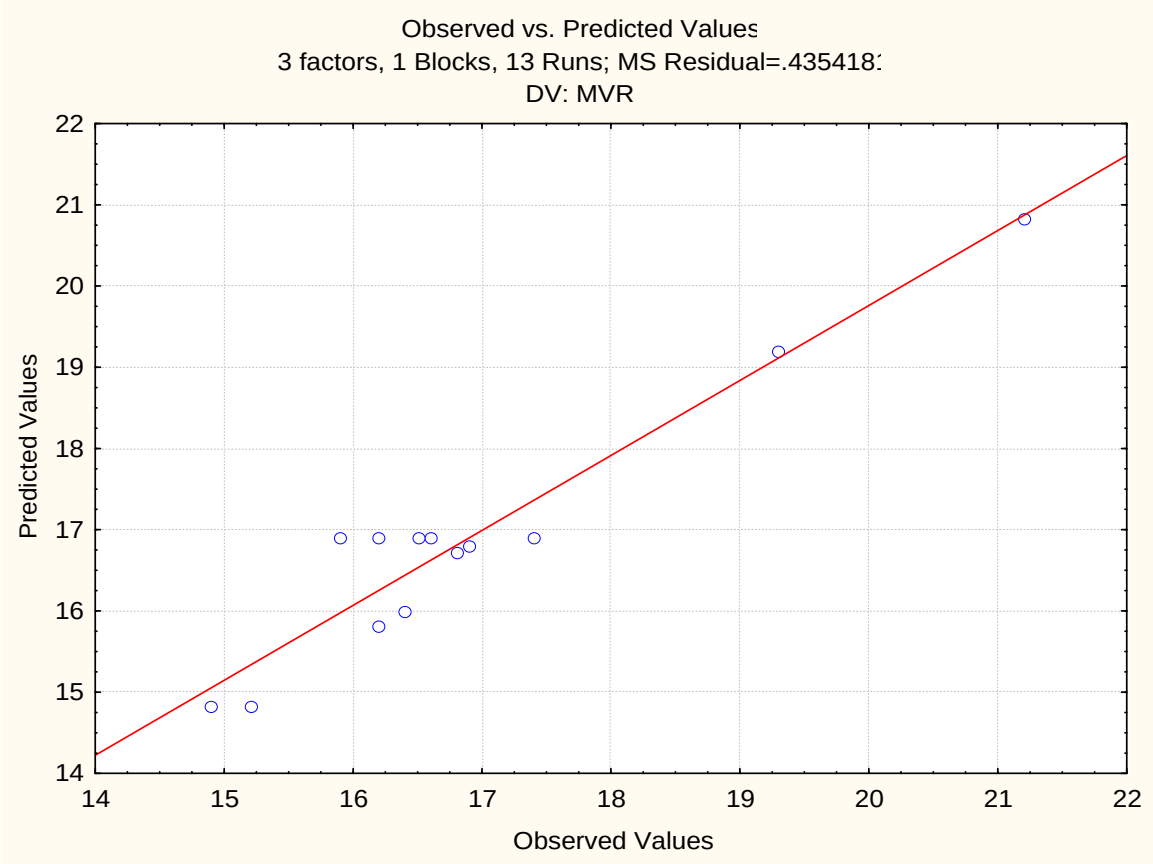

Fig. 4.1.7: Variation of predicted values with observed values of MVR for 1st set of experiments

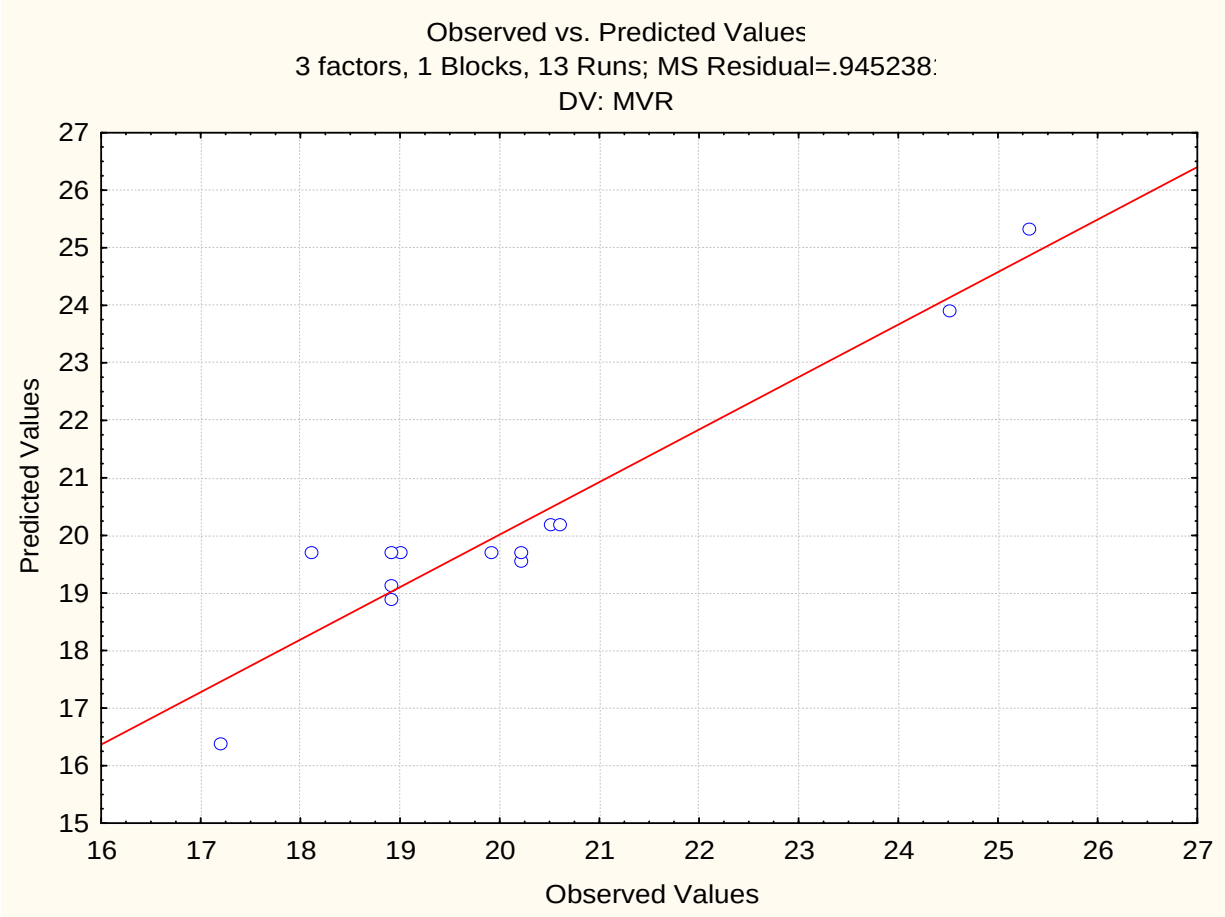

Fig. 4.1.8: Variation of predicted values with observed values of MVR for 2nd set of experiments

4.1.1.4 Three-Dimensional Response Surface Plot with Main Effects

The response surface is shown graphically in Figs. 4.1.9 and 4.1.10 for the 1st set of experiments. Both figures indicate that MVR increases as PBT flow rate increases and PC flow rate decreases. MVR values are significantly affected by the higher value of screw speed (N) than the lower

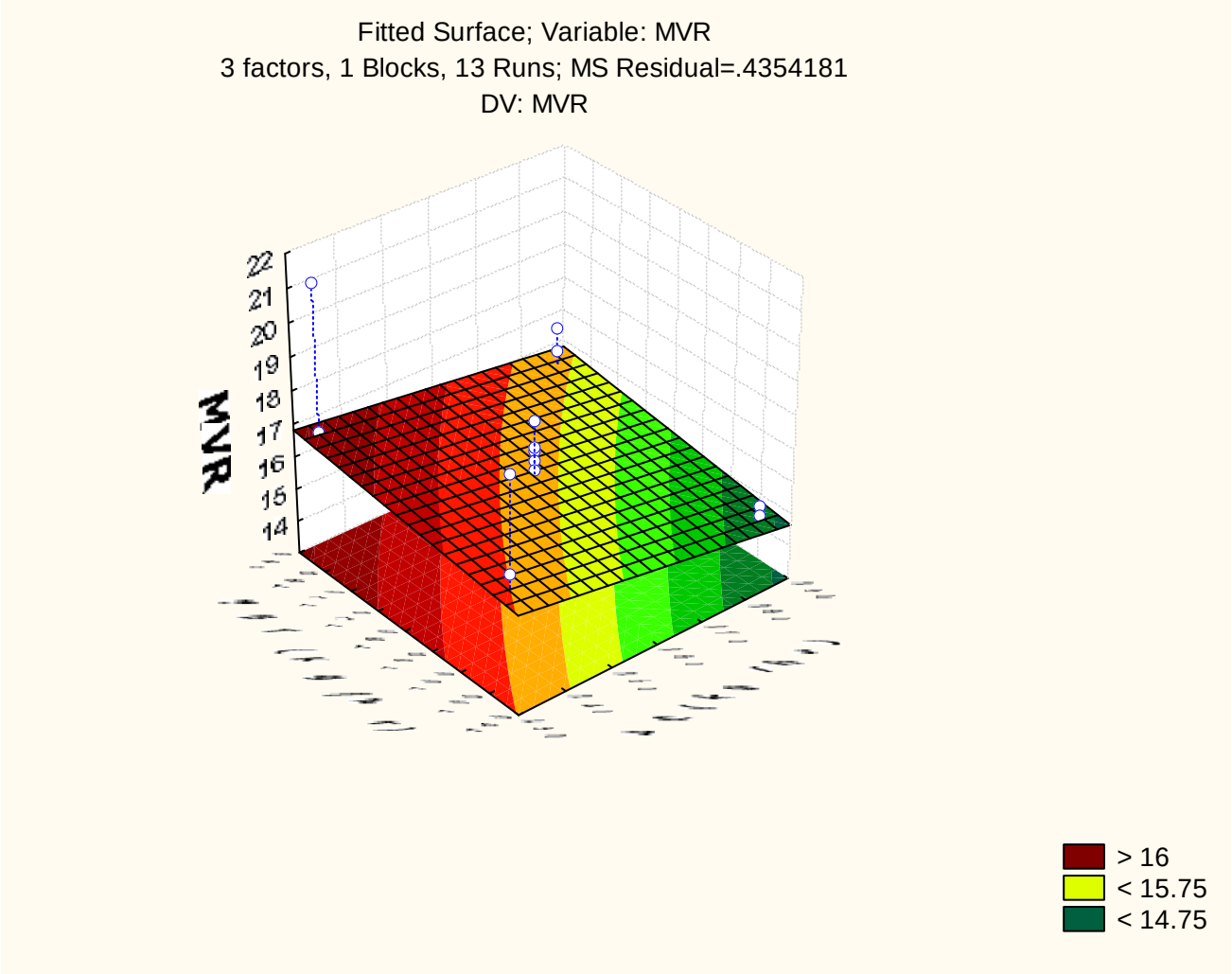

Fig. 4.1.9 : Three-dimensional response surface plot showing main effects of the two factors PC flow rate and PBT flow rate with the lowest screw-speed (N) 369 rpm on MVR of 1st set of experiments

value of screw speed (N) with different flow rate of PC and PBT. In Fig. 4.1.9, five centre points are shown in the middle of the response surface. Same trends are shown in Figs. 4.1.11 and 4.1.12 for the 2nd set of experiments.

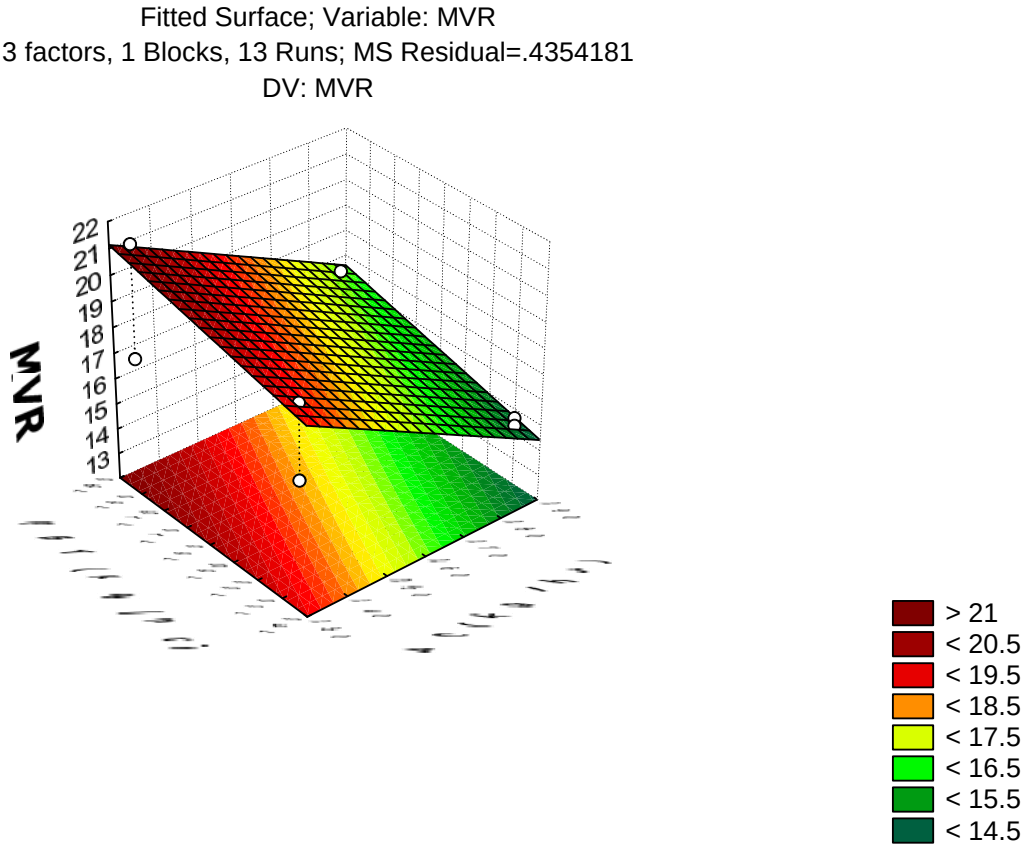

Fig. 4.1.10 : Three-dimensional response surface plot showing main effects of the two factors PC flow rate and PBT flow rate with the highest screw-speed (N) 451 rpm on MVR of 1st set of experiments

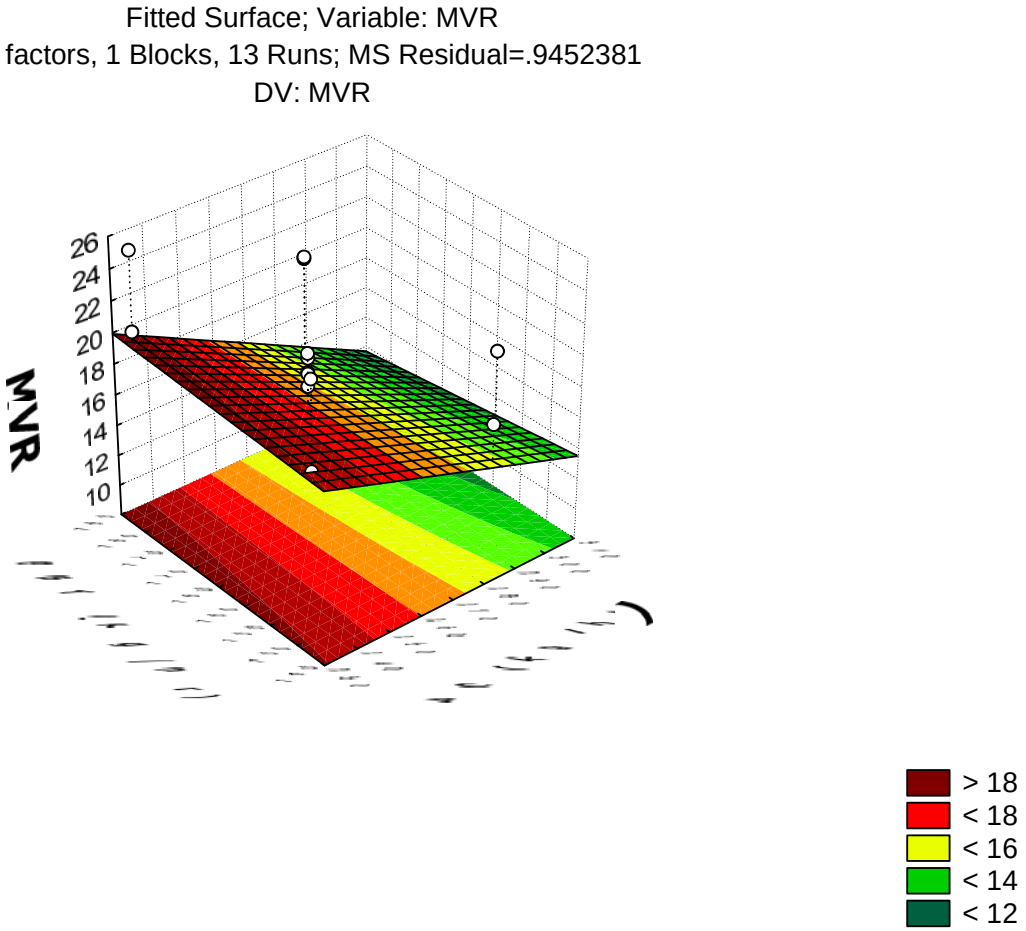

Fig. 4.1.11 : Three-dimensional response surface plot showing main effects of the two factors PC flow rate and PBT flow rate with the lowest screw-speed (N) 369 rpm on MVR of 2^{nd} sets of experiments

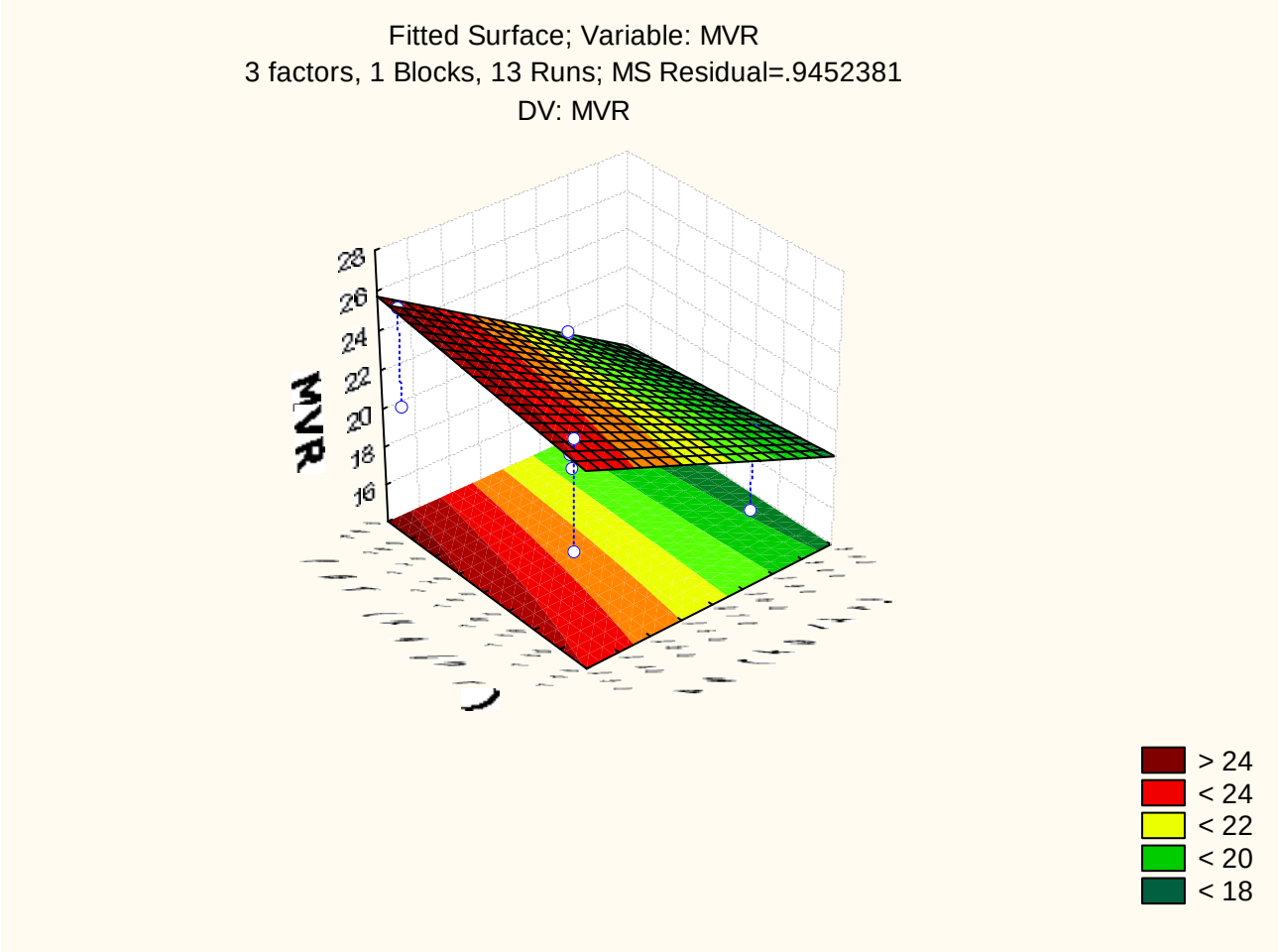

Fig. 4.1.12 : Three-dimensional response surface plot showing main effects of the two factors PC flow rate and PBT flow rate with the highest screw-speed (N) 451 rpm on MVR of 2^{nd} sets of experiments.

4.2 Dynamic Rheological Properties from Parallel Plate Rheometer

In dynamic rheometer testing, measurements were done on the last sample of each run for all three sets of experiments. That means using the sample obtained at sampling time of 19 minute of each run in the 1st set of experiments and sampling time of 15 minutes for both the 2nd and 3rd set of experiments.

As mentioned in chapter 3, the TA Rheometer (AR 2000) was used to measure the dynamic viscoelastic properties including storage modulus (G') and loss modulus (G") of PC/PBT blends. Fig.4.2.1 presents the typical response of storage modulus (G') and loss modulus (G")

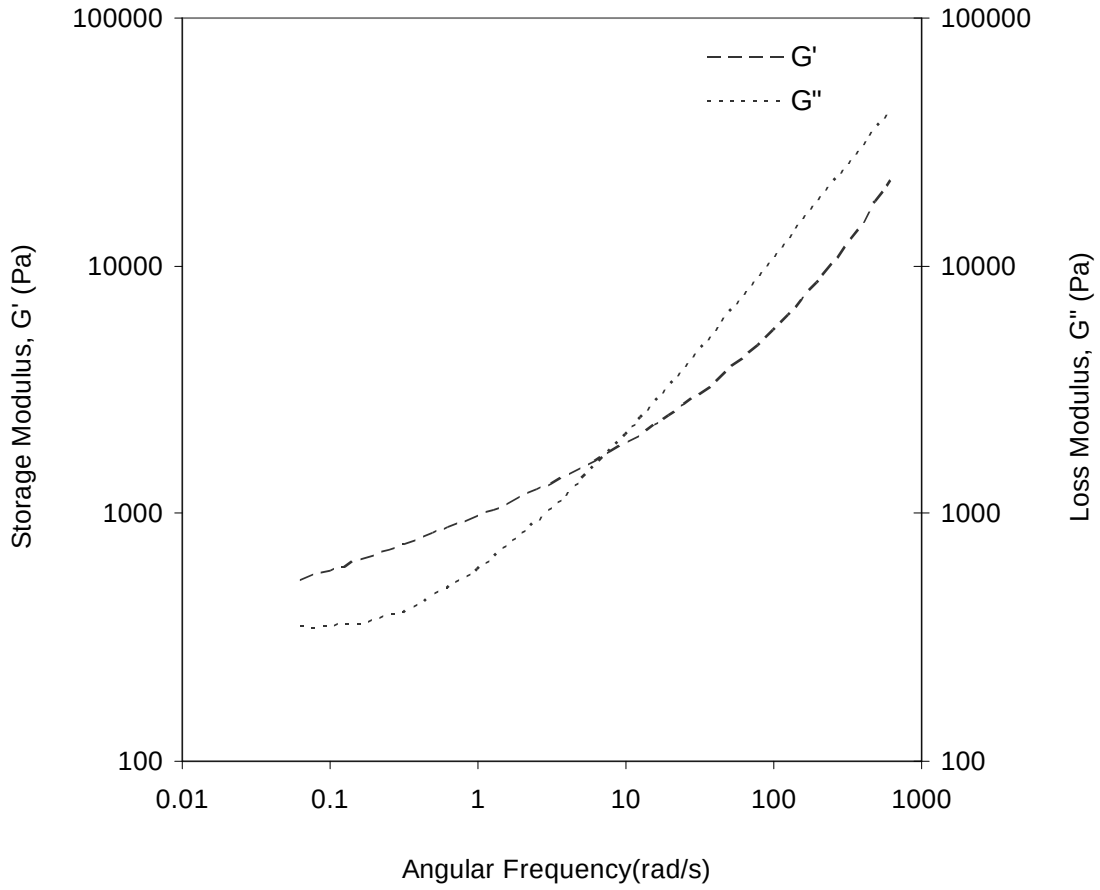

Fig. 4.2.1: Typical dynamic response behavior of PC/PBT blends of 1st set of experiments of Run1.

against angular frequency for the sample of 1st set of experiments with run number 1. Here, the slope of the loss modulus (G") curve is greater than that of storage modulus (G'). Additionally, G" is greater than G' over the range of angular frequency greater than 10 rad/s and vice versa over the angular frequency less than 10 rad/s. Here, G"> G' indicates that the viscous component of the modulus is dominant over the elastic counter part and G'> G" indicating vice versa. Same results were found for the 2nd set of experiments and more graphs were shown in Appendix.

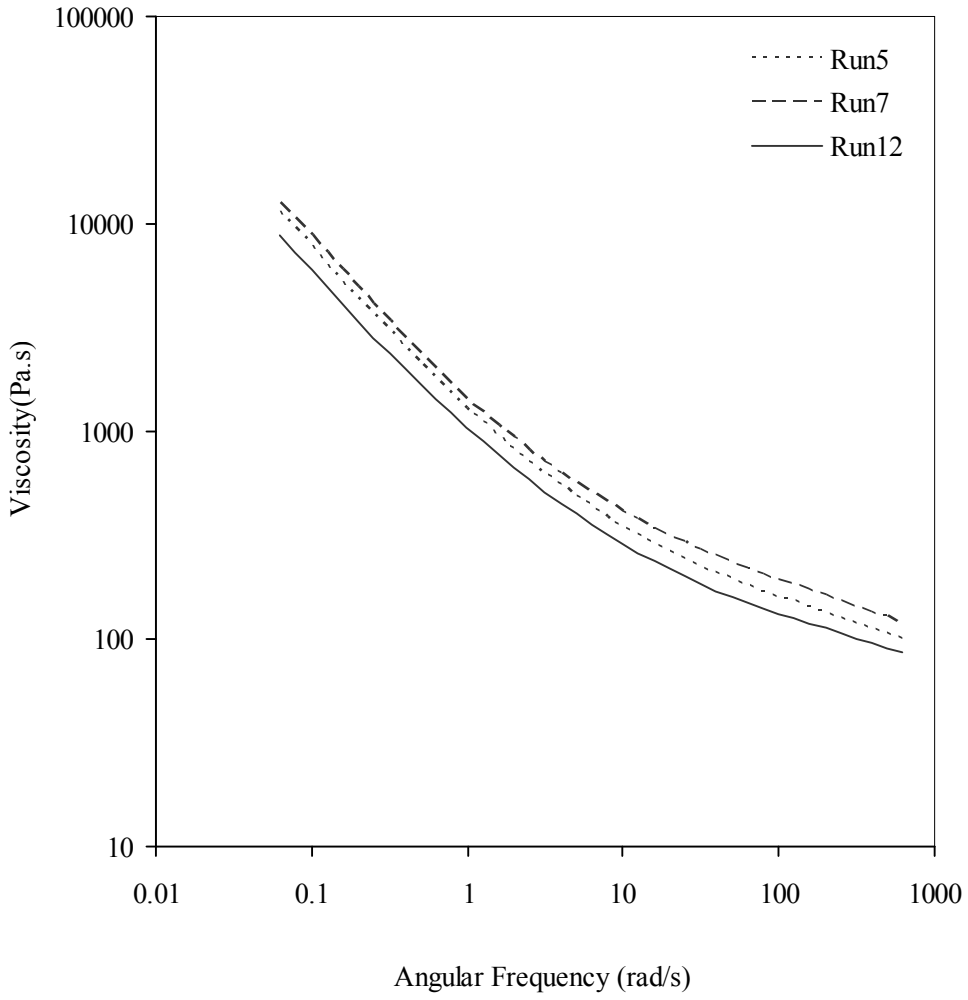

Fig. 4.2.2: Variation of viscosity with respect to angular frequency of 1st set of experiments

Fig. 4.2.2 shows the variation of viscosity with angular frequency for runs 5, 7 and 12 of the 1st set of experiments. Here, the compositions of PC in run numbers 5, 7 and 12 were 0.61, 0.66 and 0.56, respectively. From Fig. 4.2.2, it is clear that the viscosity increases with increasing concentration of PC. Also, similar behavior is observed when loss modulus versus storage modulus is compared in Fig.4.2.3.

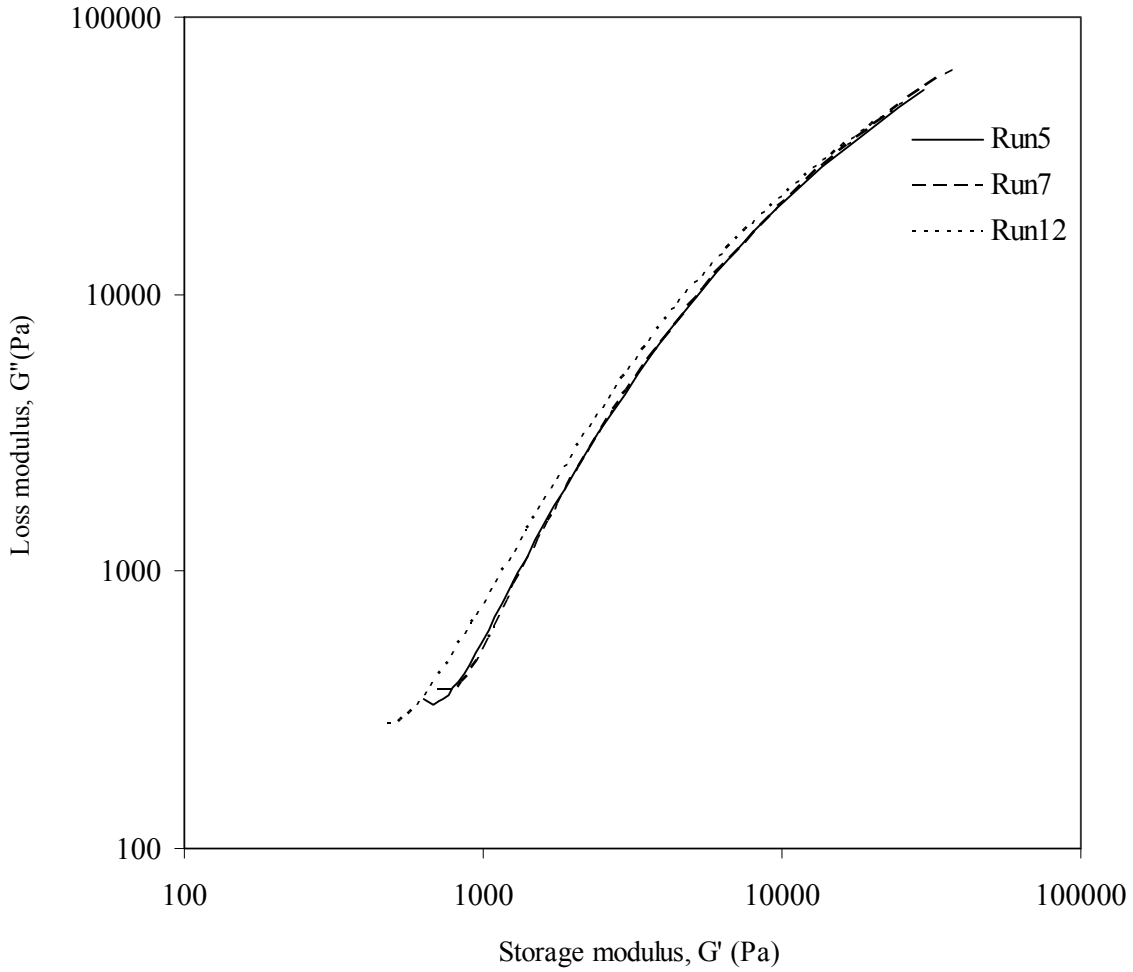

Fig. 4.2.3: Loss modulus versus storage modulus of PC/PBT blends of 1st set of experiments.

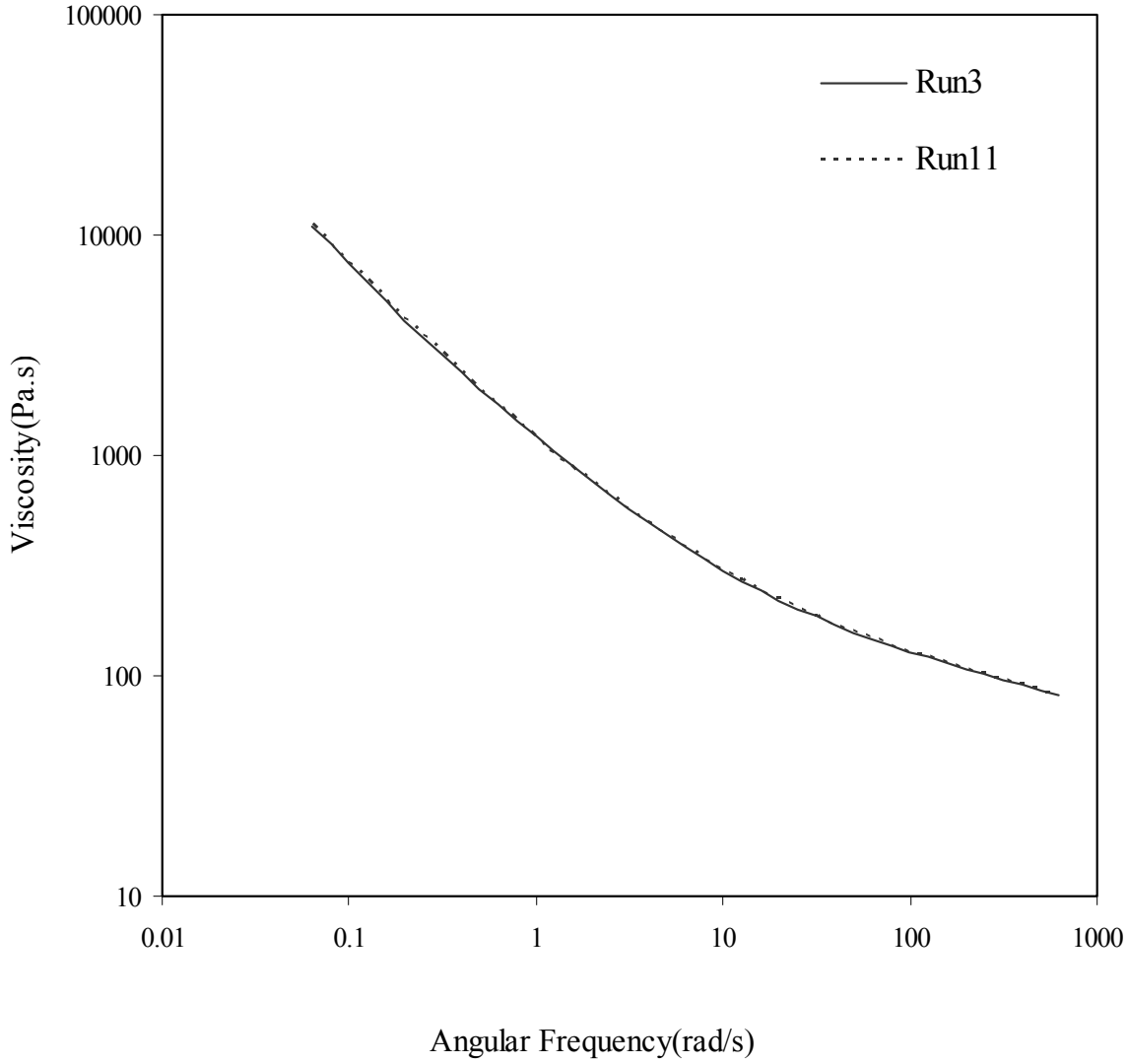

Fig. 4.2.4: Change of viscosity with respect to angular frequency of PC/PBT blends of 2nd set of experiments.

In this study, the viscosity depends on mainly the composition of PC rather than the variation of screw speed and flow rate. Fig. 4.2.4 demonstrates the variation of viscosity with angular frequency for runs 3 and 11 of the 2nd set of experiments. In these two runs, the compositions

of PC (0.61) and PBT (0.39) were the same, but the screw speed and total flow rate were 451 and 410 rpm, and 383 and 468 kg/hr, respectively. It can be seen that both curves are superimposed with each other. This means that the viscosity of polymer blends depends on composition of PC rather than screw speed and feed rate.

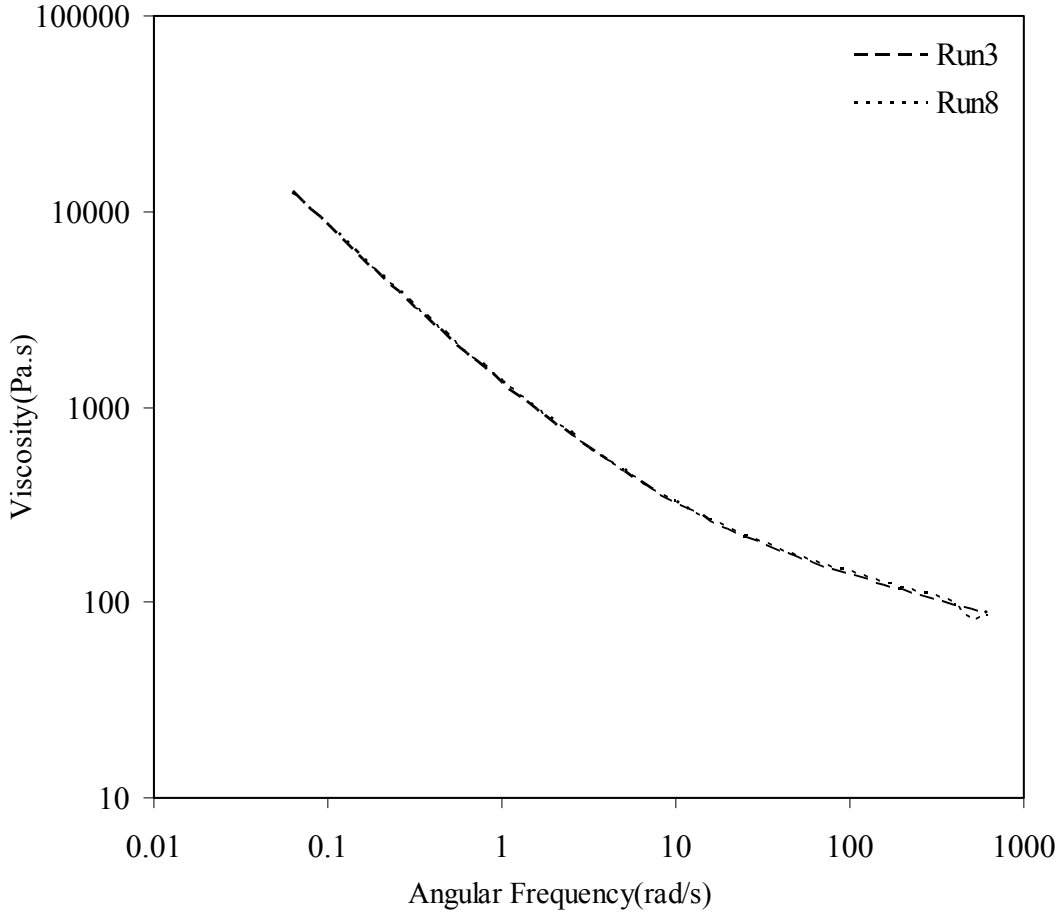

Fig. 4.2.5: Variation of viscosity with respect to angular frequency of PC/PBT blends of 1st set of experiments of Run3 and Run8.

Fig. 4.2.5 represents the variation of viscosity with angular frequency for runs 3 and 8 of the 1st set of experiments. In this two runs, the screw speed was maintained the same at 451 rpm, and also the composition of PC was 0.61 for both runs. The feed rates for runs 3

and 8 were 383 and 468 kg/hr, respectively. The viscosity curves were superimposed which indicates that the viscosity of the polymer blend does not depend on flow rate.

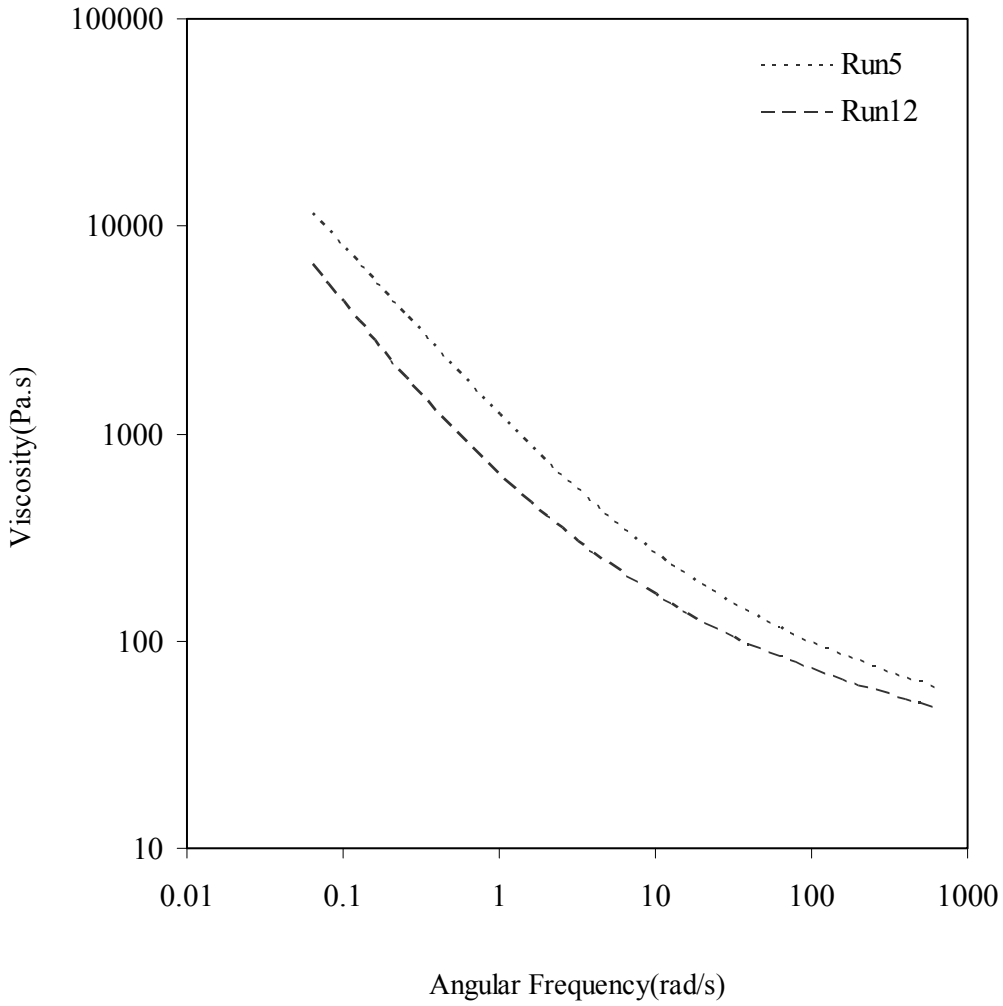

Fig. 4.2.6: Variation of viscosity with change of angular frequency of PC/PBT blends of 2nd set of experiments.

Fig. 4.2.6 shows the variation of viscosity with angular frequency for runs 5 and 12 of the 2nd set of experiments. In these two runs, the screw speed was maintained the same at

369 rpm, but the composition of PC was 0.61 and 0.56 for run 5 and 12, respectively. Also the feed rates for runs 5 and 12 were 383 and 416 kg/hr, respectively. The results show that composition of PC affects the viscosity.

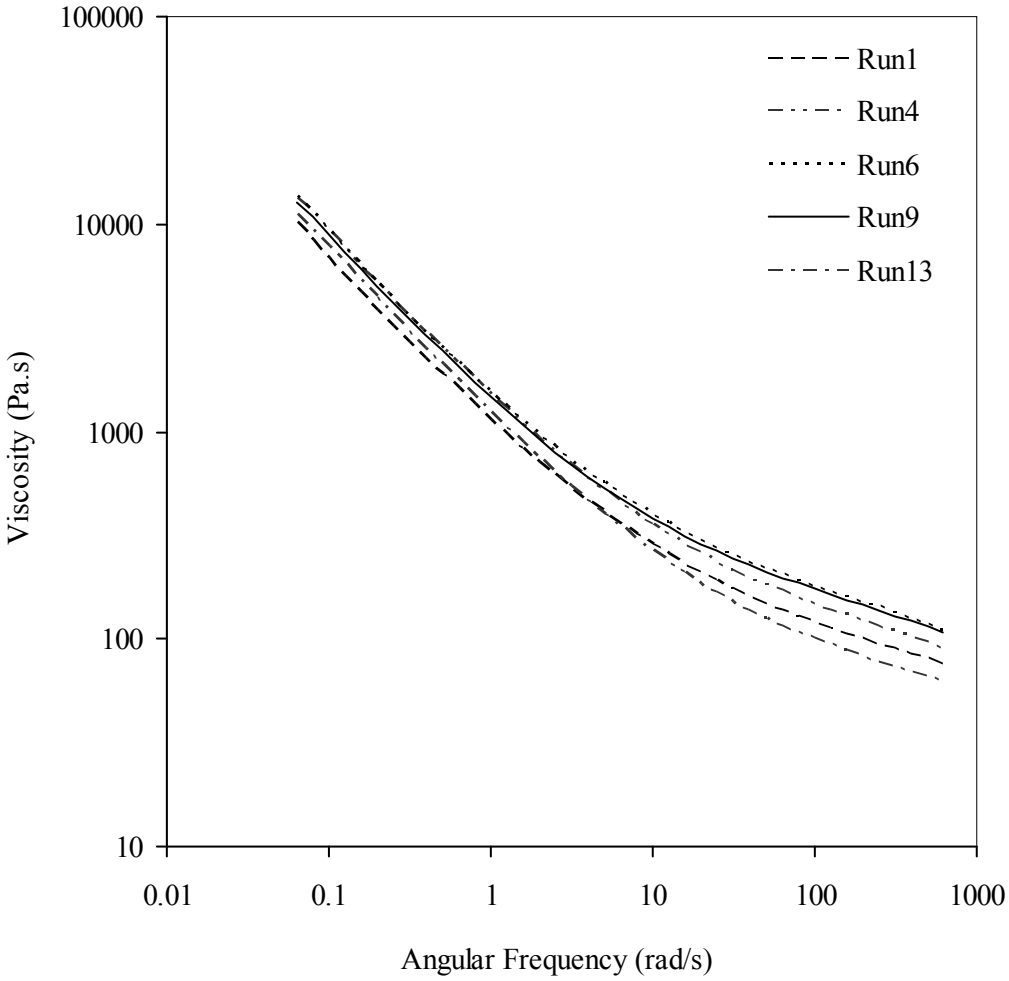

Fig. 4.2.7: Viscosity changes with variation of angular frequency of PC/PBT blends of 1st set of experiments.

The screw speed, feed rates and the composition PC for runs 1, 4, 6, 9 and 13 (centre points) of 1st and 2nd set of experiments were the same. Though all the runs had the same

variable levels, both figures 4.2.7 and 4.2.8 show different viscosity in different runs in each set of experiments. This is due to the different dies used in these sets of experiments as discussed earlier. In Figs. 4.2.7 and 4.2.8, it is shown that the viscosity values of all runs remain very close when angular frequency value is less than 1.00 rad/s and that the viscosity starts to deviate for angular frequency greater than 1.00 rad/s.

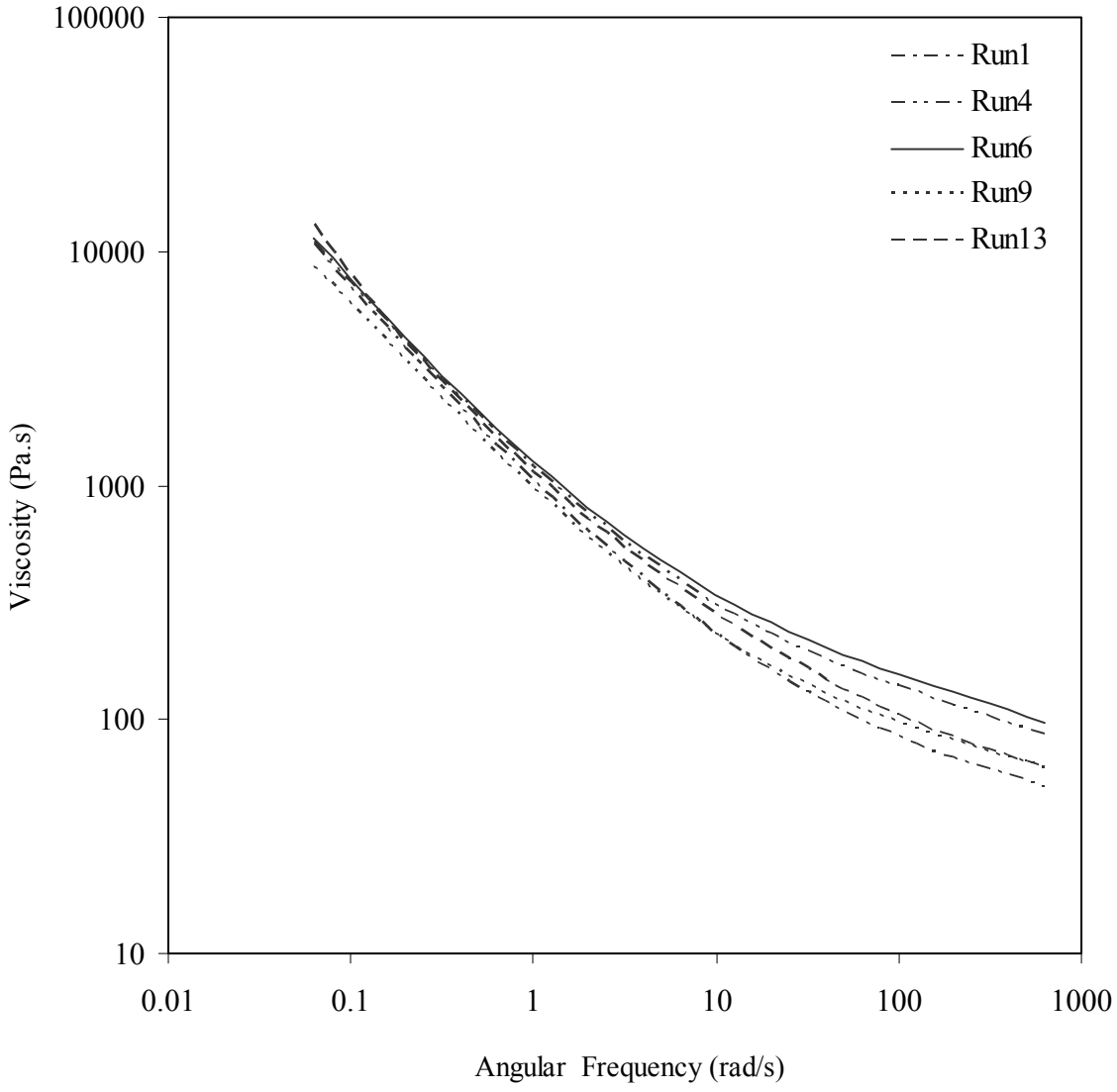

Fig. 4.2.8: Viscosity changes with variation of angular frequency of PC/PBT blends of 2nd set of experiments.

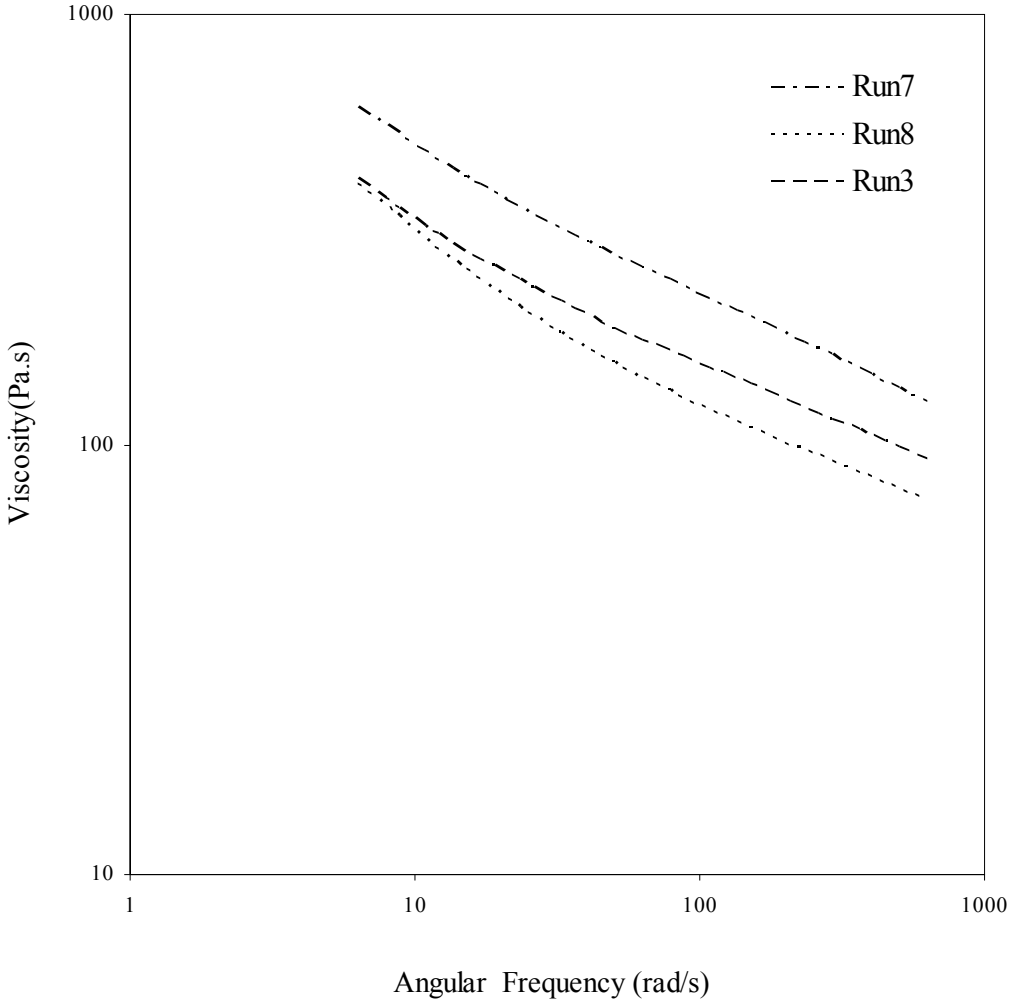

Fig. 4.2.9 : Dynamic response behavior of PC/PBT blends of 3rd set of experiments

Fig. 4.2.9 shows the viscosity with angular frequency for runs 3, 7 and 8 of the 3rd set of experiments. In the 3rd set of experiments, all nine runs were maintained at the same screw speeds (410 rpm) and total feed rates (425 kg/hr). The compositions of PC and PBT were also the same in all runs. But two types of PC were used. Compositions of PC1

in Run 3, 7 and 8 were 0.478, 0.328 and 0.528, respectively. Also compositions of PC2 in Run 3, 7 and 8 were 0.339, 0.489 and 0.289. From Fig. 4.2.9, it is shown that the concentration of the more viscous PC2 affects the viscosity of the blend.

4.3 Rheological Properties from Capillary Rheometer

The complex viscosity when plotted versus angular frequency, often superposes with steady-shear viscosity as a function of the shear rate. This is known as the Cox-Merz rule, and it provides information about a nonlinear property from a measurement of a linear property. An attempt to apply the Cox-Merz relationship to the oscillatory viscosity and capillary viscosity was not successful in these measurements.

The measurement procedure of steady-state shear viscosity, angular frequency, moduli and other related factors was described in chapter 3, section 3.2. Samples were used from both the 2^{nd} and 3^{rd} set of experiments and those were the last samples from each run in this study.

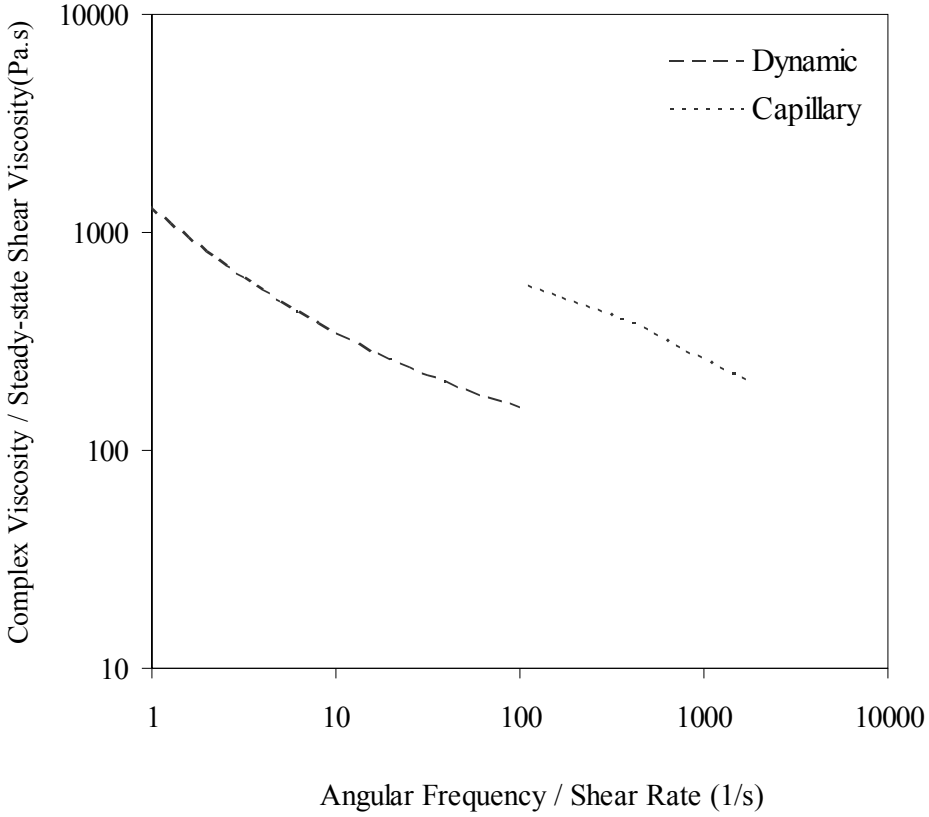

Fig. 4.3.1: Complex Viscosity / Steady-shear Viscosity as a function of Angular Frequency / Shear Rate for run number 6 of the 2nd set of experiments.

Fig.4.3.1 shows, complex viscosity / steady-shear viscosity (Pa.s) versus angular frequency / shear rate (1/s) curves of run number 6 with sampling time 15 minutes in the 2nd set of experiments. It is shown that the Cox-Merz rule is not obeyed (viz, curves do not superimpose) in PC/PBT blend case. This was repeated for other samples of the same set of experiments. Fig. 4.3.2 shows, complex viscosity / steady-shear viscosity (Pa.s) versus angular frequency / shear rate (1/s) curves of run number 13 with sampling time

15 minutes in the 2nd set of experiments. This run also shows the same trend. Samples from the 3rd set of experiments were checked as well.

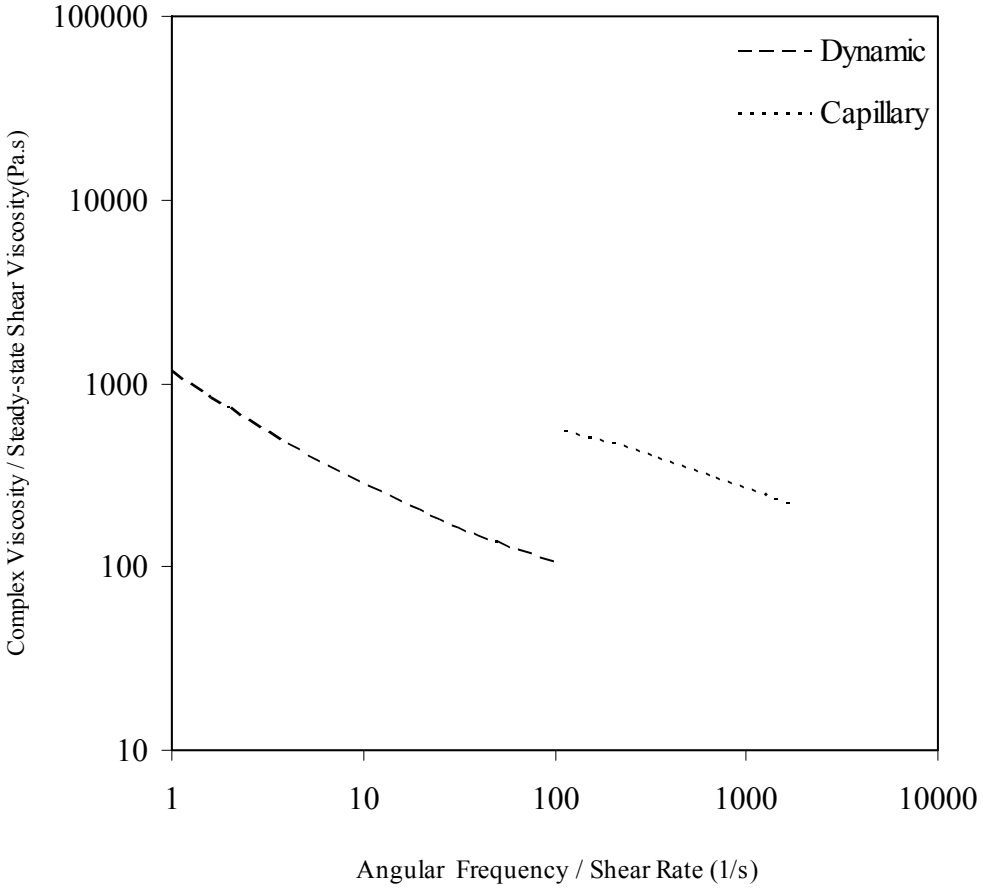

Fig. 4.3.2: Complex Viscosity /Steady-shear Viscosity as a function of Angular Frequency /Shear Rate for run number 13 of the 2nd set of experiments.

Fig.4.3.3 shows the curves of complex viscosity / steady-shear viscosity (Pa.s) versus angular frequency / shear rate (1/s) for run number 3 of the 3rd set of experiments with sampling time 15 minute. The results are similar. Also Fig. 4.3.4 represents the curves for run

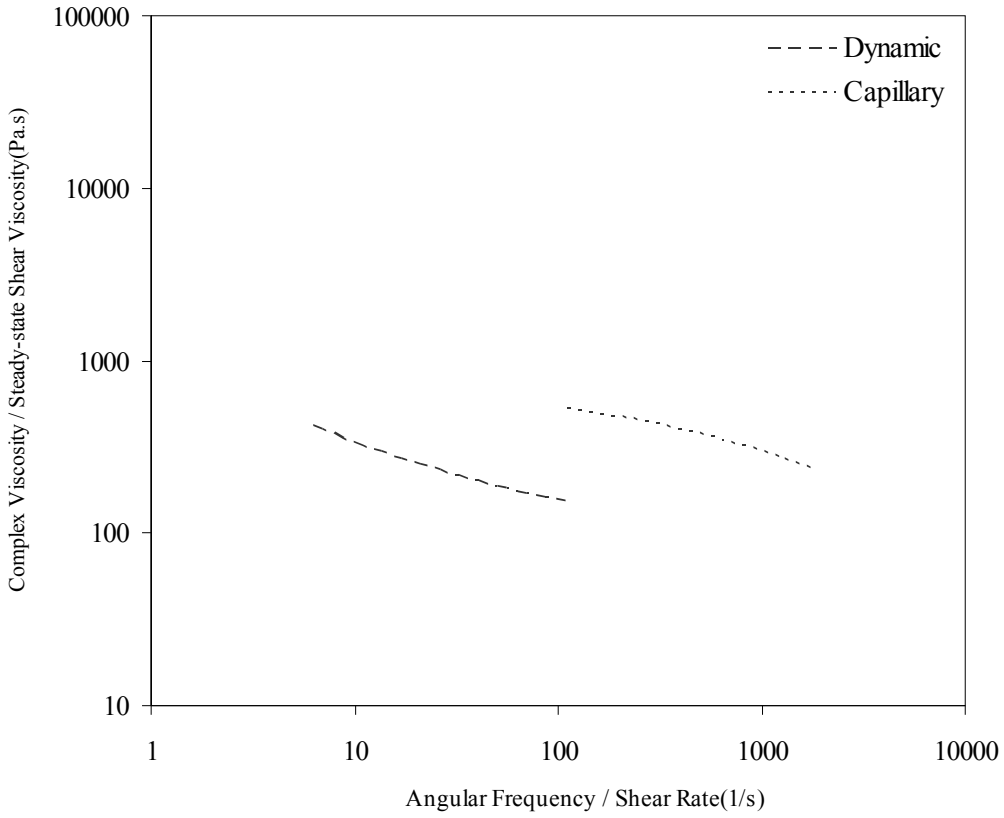

Fig. 4.3.3: Complex Viscosity /Steady-shear Viscosity as a function of Angular Frequency /Shear Rate of run number 3 of 3rd set of experiments.

number 8 of the 3rd set of experiment and the curves did not superpose. So, it is postulated that the Cox-Merz rule is not obeyed for the compounding of PC/PBT. Schulken et al. [58] suggested that polymers composed of very stiff rod like molecules may not give agreement in comparing steady state shear rate with dynamic frequency. Also, Hsieh et. al [59] concluded that the Cox Merz rule is found not to be obeyed by all the polymers studied. As pointed out by Booij et al. [60], the Cox-Merz rule is not applicable to strongly nonlinear melts. Therefore, it is not surprising that the curves do not superimpose and Cox-Merz rule is not properly obeyed in PC/PBT blends. It is noted

that more curves for complex viscosity / steady-shear viscosity as a function of angular frequency / Shear Rate were shown in Appendix of this thesis.

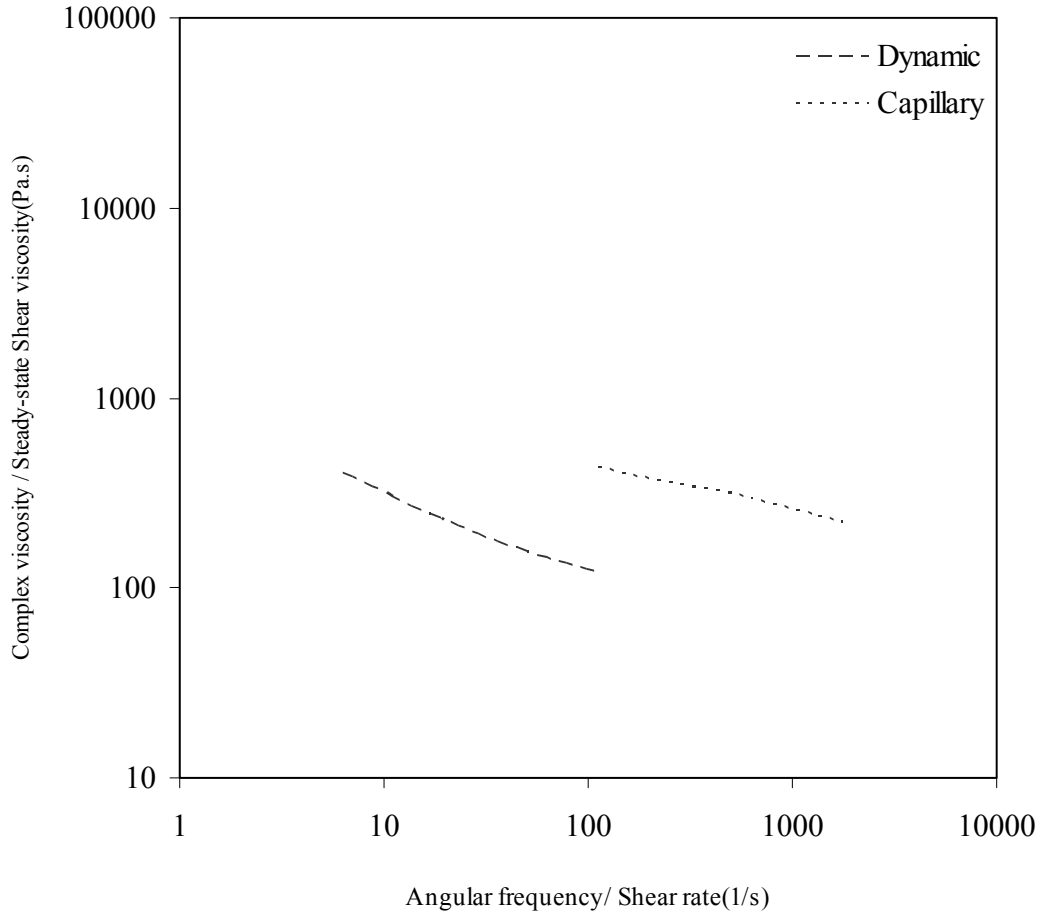

Fig. 4.3.4: Complex Viscosity /Steady-shear Viscosity as a function of Angular Frequency /Shear Rate of run number 8 of the 3rd set of experiments.

4.4 Scanning Electron Microscopy (SEM) Results

Changes in the morphology of PC/PBT blends were studied under a scanning electron microscopy (SEM). The SEM experimental procedure was described in chapter 3 and samples were used from the 2nd set of experiments of run number 13 at 10 minute time intervals. Both stained and unstained samples were used to compare the SEM photographs. Images from the Reel Back-Scattering Electron (RBSE) detector and Secondary Electron (SE) detector were taken for the element and topological contrast. The morphology depends strongly on composition, with bi-continuous morphologies usually observed at near critical composition, where PC and PBT can dissolve in each other in their blend [4]. Wu at el. [61] postulated that a 50/50 (PC/PBT) blend possessed a bicontinuous structure and the other blends had a dispersed phase of either PBT or PC depending on which was the minor component. In this study, PBT was the minor component and a dispersed phase of PBT in PC was found. It is noted that sample's compositions of PC and PBT were 61% and 39%, respectively.

Fig. 4.4.1 shows unstained samples and there is no significant difference in morphology of all three (a), (b) and (c) SEM micrographs.

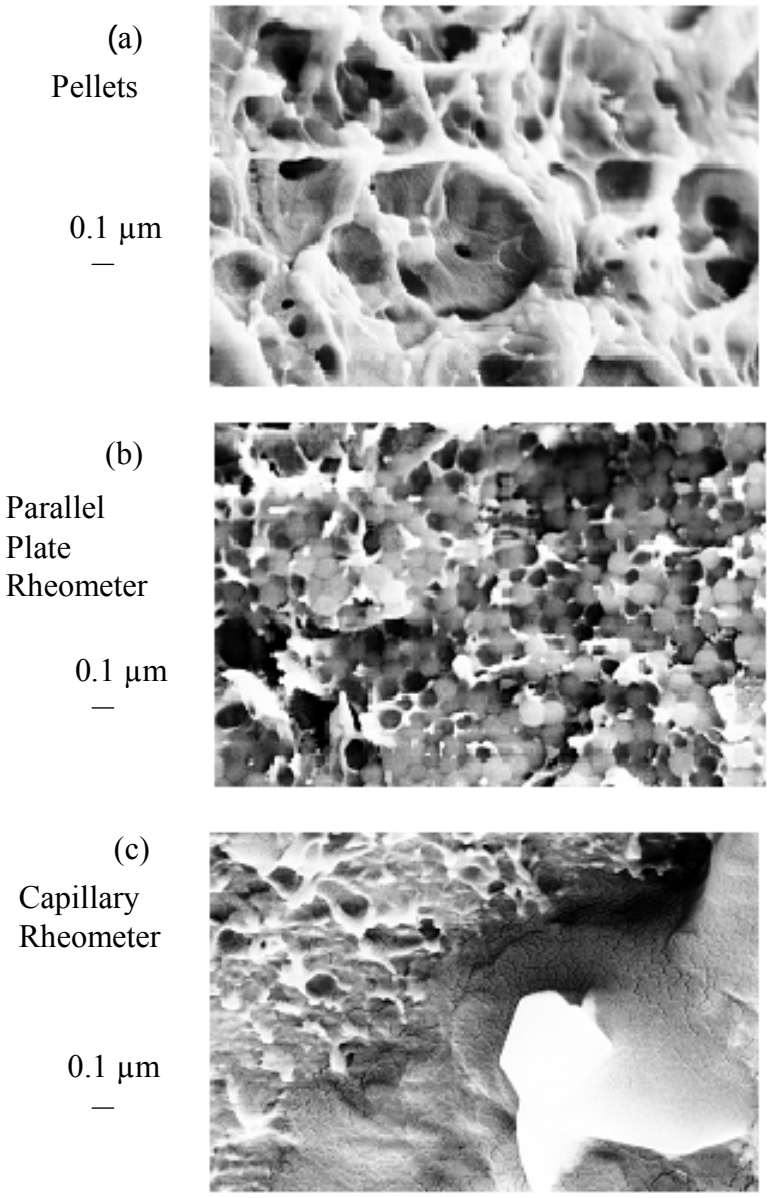

Fig. 4.4.1 : SEM micrographs of unstained samples

Fig. 4.4.2 also shows the images of unstained samples and there was some difference between the morphology of pellets and samples collected after completing the tests both in parallel and capillary rheometers. The samples collected after completing the test in parallel and capillary rheometers may have degraded. After completing the tests in

parallel and capillary rheometers, the samples' morphology may have changed due to degradation of PC/PBT blends. Same behavior was found in Fig. 4.4.3 where samples were stained by RuO_4.

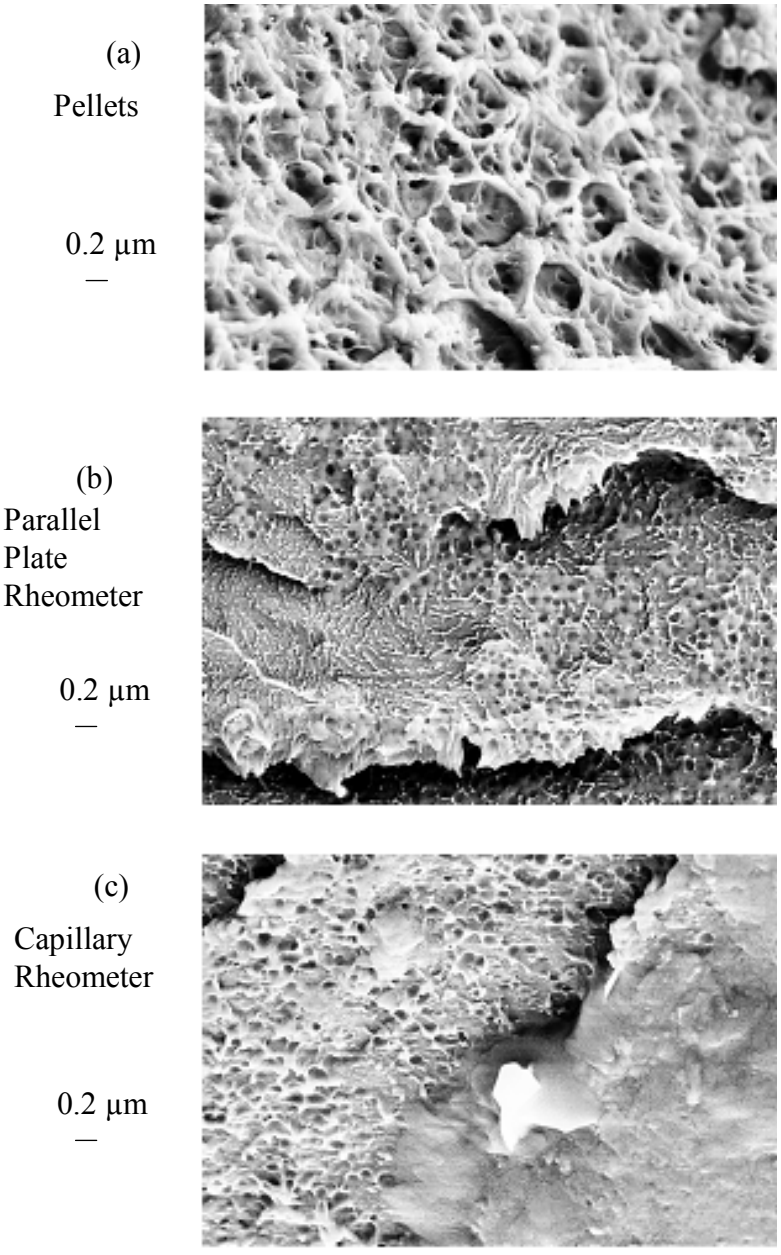

Fig. 4.4.2 : SEM photographs of unstained samples

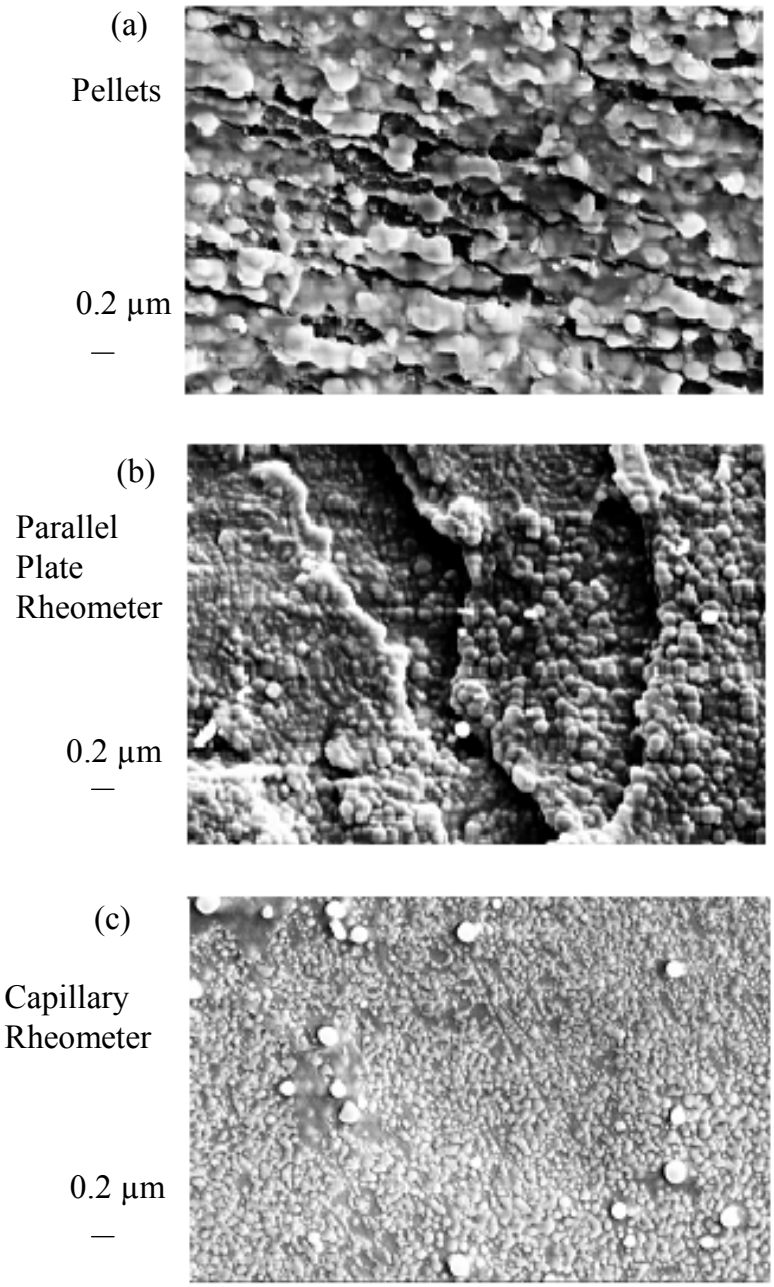

Fig. 4.4.3 : SEM micrographs of stained samples

Since diffusion of ruthenium tetroxide (RuO_4) vapor in the amorphous region would be expected to occur more readily than that in the crystalline region [62]. The dark stained lines in Figs.4.4.3 and 4.4.4 are probably the amorphous areas between crystallites. Also, Wu et al. [61] demonstrated that the black continuous phase is PC which was stained by RuO_4. And also white dispersed particles are PBT, which were quite randomly and uniformly distributed in the PC matrix.

The SEM photographs from the reel backscattering electron detector (RBSD) of the same samples stained by RuO_4 have dominant information about element composition as shown in Figure 4.4.5. No significant differences in morphology observed among the samples.

Fig. 4.4.6 shows the morphology of RBSD stained by RuO_4. There is no significant difference among the three images.

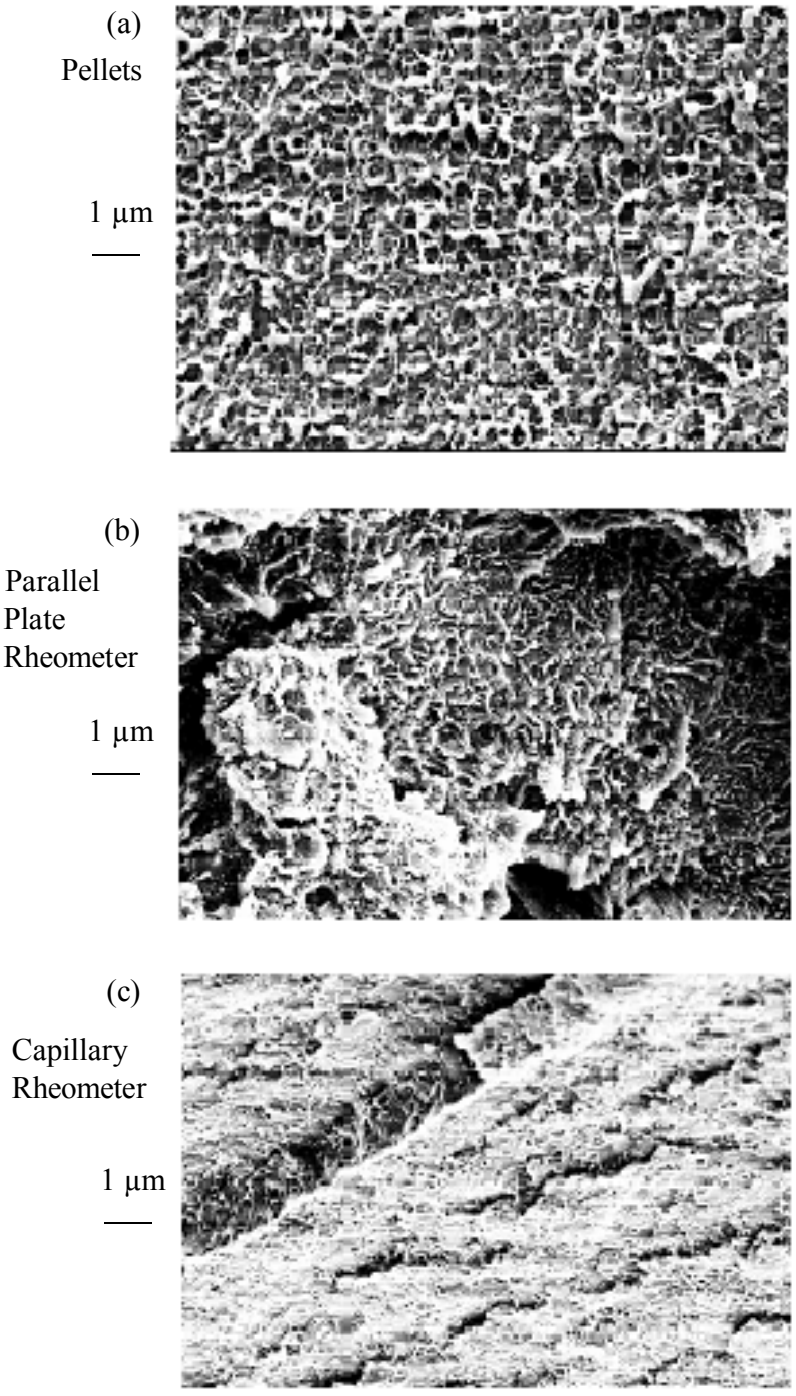

Fig. 4.4.4 : SEM micrographs of stained samples

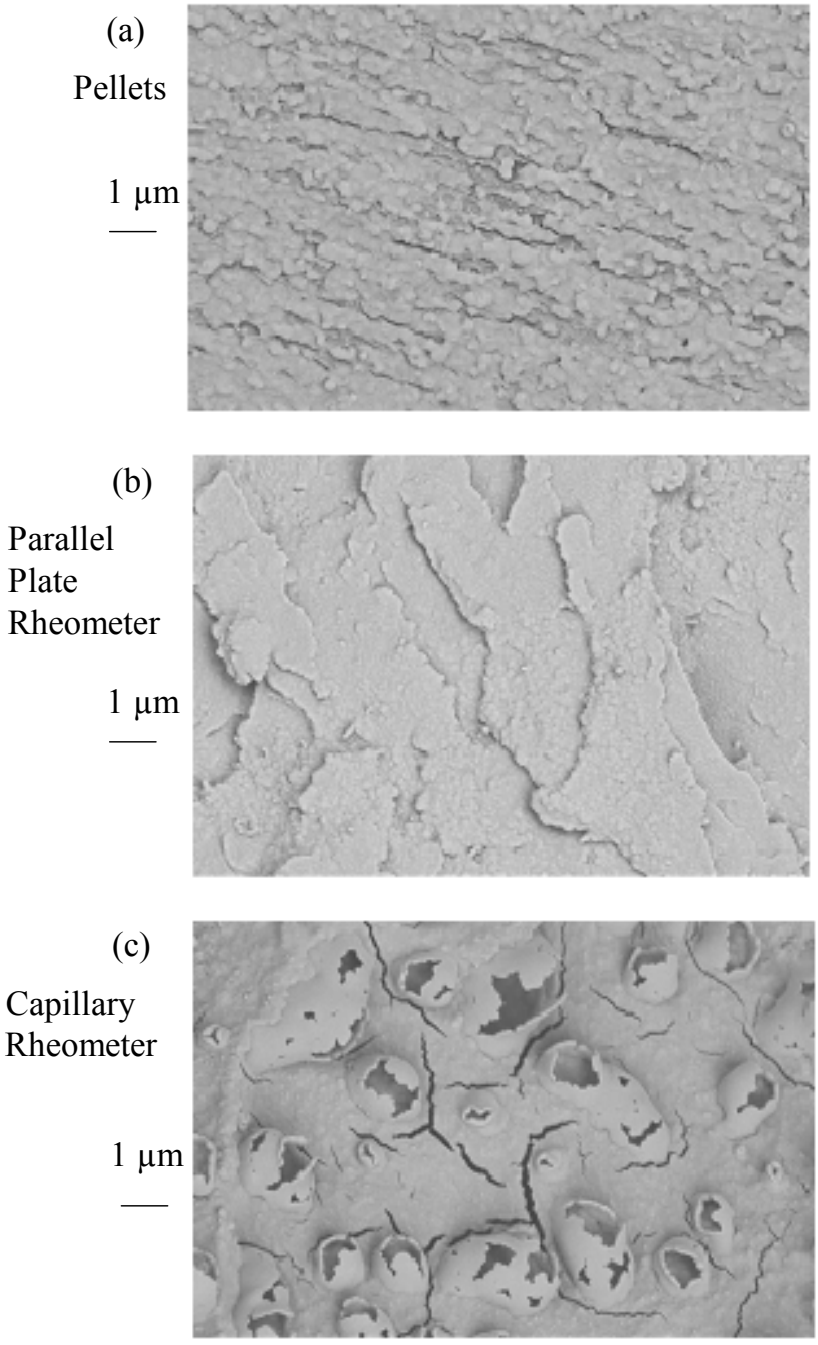

Fig. 4.4.5 : SEM photographs from the reel backscattering electron detector (RBSD)

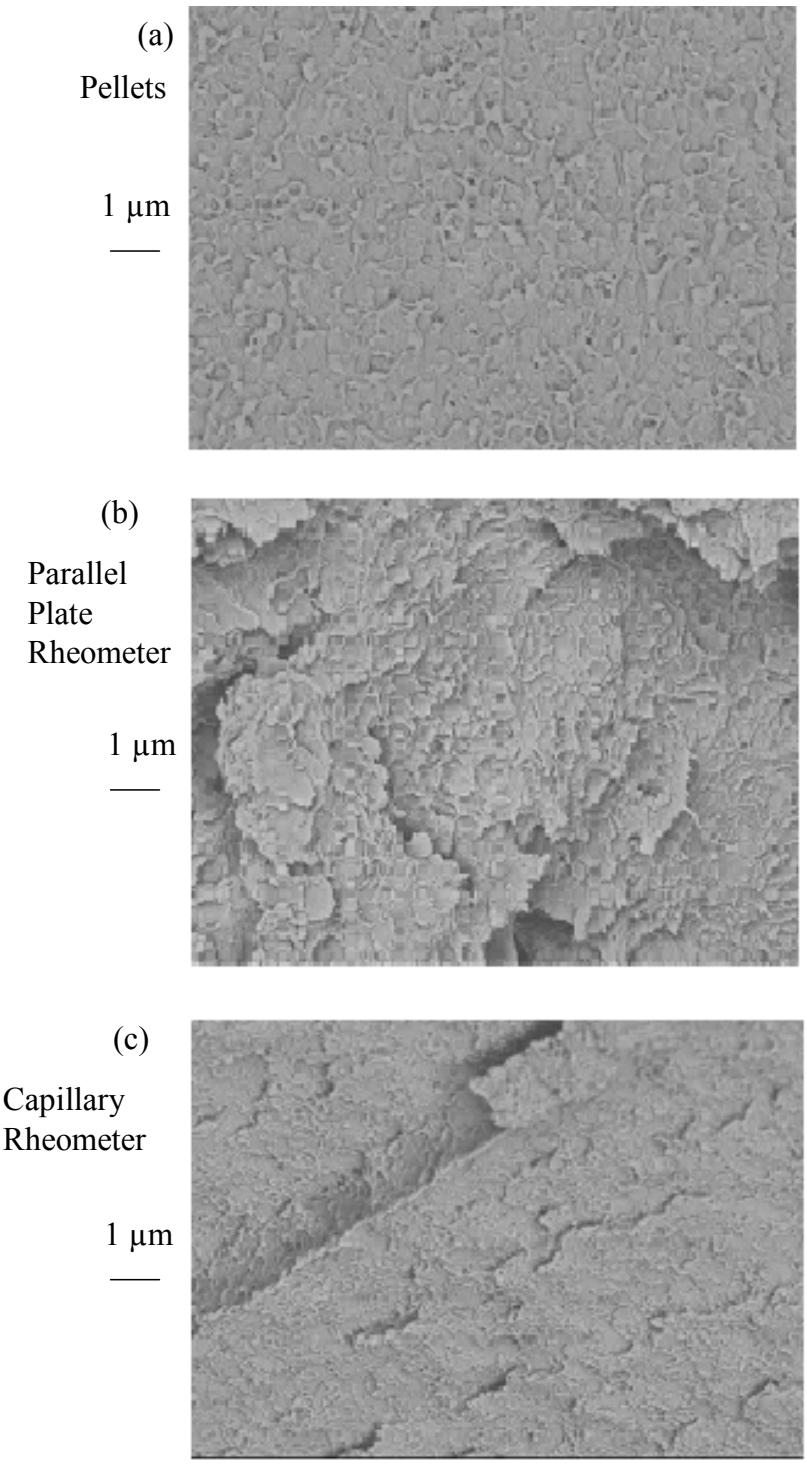

Fig. 4.4.6 : SEM images from the reel backscattering electron detector (RBSD) stained by RuO_4

Chapter 5
CONCLUSIONS AND RECOMMENDATIONS

The objective of this work was to improve the quality of products of PC/PBT blends regarding customer satisfaction, minimized waste product and maximized profit. Melt Volume-Flow Rate (MVR) is the quickest method to find out the flow characteristics of blends. It measures the flowability of thermoplastic polymers and gives an indication of the flow properties of the melt, thus indicating processing qualities of polymer.

Variations of MVR with sampling times were studied. The screw speeds were increased with time at constant feed rates of PC and PBT. It was shown that when the feed rates increased, MVR decreased due to decrease of average residence time. Higher screw speed resulted in higher MVR value at constant feed rate and increased flow rate resulted in lower residence time that leads to reduced MVR. The measurements of MVR data were statistically analyzed by analysis variance (ANOVA).

Dynamic rheological properties from parallel plate rheometer measurement were shown that the polymer blends viscosity increased with increasing the concentration of PC. The experimental results showed that viscosity of polymer blends depends on the composition of PC rather than the variations of screw speed and feed rates. Here, experiments were done with constant screw speeds or constant feed rates or constant PC compositions as well as with different screw speeds or different screw speeds or different PC compositions.

An attempt to apply the Cox-Merz relationship to the oscillatory viscosity and capillary viscosity was not successful in this study. So, it would be concluded that Cox-Merz rule was found not to be obeyed by all the polymers studied.

The samples collected after completing the tests in parallel and capillary rheometers may be degradable when studied under scanning electron microscope (SEM). The samples with stained by RuO_4 showed evidence that RuO_4 reacted strongly with PBT, possibly leading to cross linking of PBT.

5.1 Recommendation for Path Forward

In this work, the 1st and 2nd sets of experiments were done by a 2^3 factorial design of experiments and due to machine operating limitations, some of the combinations of the levels were not feasible and were adjusted to practical levels of the factors studied. Minimizing machine operating limitation could be a future task of this works.

Changes in the morphology of PC/PBT blends were studied under a scanning electron microscope (SEM). In this study, samples were used only from 2nd set of experiments of run 13 with a 10 minute time interval. So, more study has to be done on the other sets of experiments to compare the morphology and highlight the effect of all processing variables.

The measurements of MVR data were statistically analyzed by analysis of variance (ANOVA). More statistical analysis needs to be done in the future and the results need to be evaluated against actual production data that are not well controlled.

REFERENCES

1. A. Ajji , L. A. Utracki, "lnterphase and Compatibilization of Polymer Blends", Polym. Eng. Sci., 36, 1574-1585 (1996)

2. S. C. Tjong ,Y. Z. Meng, "Properties of Ternary In Situ Polycarbonate / Polybutylene Terephthalate /Liquid Crystalline Polymer Composites", J. Appl. Polym. Sci, 74, 1827-1835 (1999)

3. C-K. Shih , C-K. Shih, L.L.C., "Innovations in Selected Commercially Significant Polymer Blend and Blending Process", SPE ANTEC Technical Papers (2002)

4. J. M. R. C. A. Santosa, J. T. Guthrie, "Polymer blends: the PC–PBT case", J. Mater. Chem., 16, 237-245 (2006)

5. W. Birley, X.Y. Chen, "Further studies of polycarbonate-poly(butylene terephthalate) blends" , Br. Polym. J., 17, 297-305 (1985)

6. R. S. Halder, M. Joshi, A. Misra," Morphological studies on the blends of poly (butylenes terephthalate) and bisphenol-A polycarbonate", J. Appl. Polym. Sci., 39, 1251-1264 (1990)

7. D. C. Wahrmund, D. R. Paul, J. W. Barlow, "Polyester-polycarbonate blends. I. Poly(butylene terephthalate)", J. Appl. Polym. Sci., 22, 2155-2164 (1978)

8. P. Sanchez, P. M. Remiro, J. Nazabal, "Physical properties and structure of unreacted PC/PBT blends", J. Appl. Polym. Sci., 50, 995-1005 (1993)

9. K. J. Lee, J. M. Kim, J. G. Kum, J. M. Oh, "Phase behavior of bisphenol-A polycarbonate and poly(ester-ether) elastomer blend", SPE ANTEC Technical Papers, 2458-2465 (1998)

10. P. Marchese, A. Celli, M. Fiorini, "Relationships between the molecular architecture, crystallization capacity, and miscibility in poly(butylenes terephthalate) / polycarbonate blends : A comparison with poly(ethylene terephthalate) / polycarbonate blends" , J. Polym. Sci.: Part B: Polym. Phys., 42, 2821-2832 (2004)

11. G. Pompe, L. Haubler, "Investigations of Transesterification in PC/PBT Melt Blends and the Proof of Immiscibility of PC and PBT at Completely Suppressed Transesterification", J. Polym. Sci.: Part B: Polym. Phys., 35, 2161-2168 (1997)

12. J. Devaux, P. Godard, J. P. Mercier, "The transesterification of bisphenol-a polycarbonate(PC) and polybutylene terephthalate (PBT): A new route to block copolycondensates", J. Polym. Eng. Sci., 22, 229-233 (1982)

13. A. N. Wilkinson , S. B. Tattum, "Melting reaction and recrystallization in a reactive PC-PBT blend", Polymer, 38, 1923-1928 (1997)

14. S. B. Tattum, D. Cole, A. N. Wilkinson," Controlled Transesterification and Its Effects on Structure Development in Polycarbonate-Poly(Butylene Terephthalate) Melt Blends" , J. Macromol. Sci., Part B, 39, 459-479 (2000)

15. I. Hopfe, G. Pompe and K.J. Eichhorn, "Ordered structures and progressive trans-esterification in PC/PBT melt blends studied by FTIR. spectroscopy combined with DSC and n.m.r.", Polymer, 38, 2321-2327 (1997)

16. E. M. S. Sanchez, "Ageing of PC/PBT blends : Mechanical properties and recycling possibility", Polym. Testing, 26, 378-387 (2007)

17. L. A. Utracki, "Compatibilization of Polymer Blends", Can. J. Chem. Eng., 80, 1008-1016 (2002)

18. S. P. Mishra, P. Venkidusamy, "Structural and thermal behavior of PC/PBT blends", J. Appl. Polym. Sci., 58, 2229 - 2234 (1995)

19. S. S. Pesetskii, B. Jurkowski, V. N. Koval, "Polycarbonate/polyalkylene terephthalate blends: Interphase interactions and impact strength", J. Appl. Polym. Sci., 84, 1277-1285 (2002)

20. T. W. Tseng, J. S. Lee," Functional MBS impact modifiers for PC/PBT alloy", J. Appl. Polym. Sci., 76, 1280 - 1284 (2000)

21. B. J. Reekmans, K. Nakayama, "Hot drawing of partially miscible blends of polycarbonate and poly(butylene terephthalate)", J. Appl. Polym. Sci., 62, 247 - 255 (1996)

22. D. Delimoy, B. Goffaux, J. Devaux, R. Legras, "Thermal and morphological behaviors of bisphenol A polycarbonate / poly (butylene terephthalate) blends", Polymer, 36, 3255-3266 (1995)

23. A. C. M. V. Bennekom, D. V. D. Berg, J. Bussink and R. J. Gaymans, "Blends of amide modified polybutylene terephthalate and polycarbonate : phase separation and morphology", Polymer, 38, 5041 - 5049 (1997)

24. S. Y. Hobbs, M. E. J. Dekkers and V. H. Watkins, "The morphology and deformation behavior of poly (butylene terephthalate)/BPA polycarbonate blends", Polym. Bul., 17, 341-345 (1987)

25. S. Nabar, D. D. Kale, "Rheology and transesterfication between polycarbonate and polyesters", J. Appl. Polym. Sci., 104, 2039-2047 (2007)

26. J. Wu, K. Wang, D. Yu, "Fracture toughness and fracture mechanisms PBT/PC/IM blend", J. Mater. Sci., 38, 183-191 (2003)

27. H. Bai, Y. Zhang, Y. Zhang, X. Zhang, W. Zhou, "Toughening modification of PBT/PC blends by PTW", Polym. Testing, 24, 235-240 (2005)

28. S. Y. Hobbs, V. L. Groshans, M. E. J. Dekkers, A. R. Shultz, "Partial miscibility of poly (butylene terephthalate)/BPA polycarbonate melt blends", Polym. Bul., 17, 335-339 (1987)

29. W. S. Depolo, D. W. Litchfield, D. G. Baird, "Rheological characterization of compatibility & degradation of polycarbonate / polybutylene terephthalate layered silicate nanocomposities", Antec Papers, 2330-2334 (2006)

30. A. Rudin, "The Elements of Polymer Science and Engineering", Second Edition, Academic Press, USA(1999)

31. J. M. Dealy, S. S. Soong, "A Parallel Plate Melt Rheometer Incorporating a Shear Stress Transducer", J. Rheol., 23, 355-365 (1984)

32. J. M. Dealy and K.F. Wissburn, "Melt Rheology and its Role in Plastics Processing", Van Nostrand Reinhold, New York (1990)

33. C. A. Braybrook, J. A. Lee and P. J. Bates, "Measurement of the high frequency viscoelastic properties of polypropylene using a sliding plate rheometer", Antec Papers, 1970-1972 (2007)

34. W. P. Cox, E. H. Merz, "Correlation of dynamic and steady flow viscosities", J. Polym. Sci., 28, 619-622 (1958)

35. G. Goizueta, T. Chiba and T. Inoue, "Phase morphology of polymer blends: 2. SEM observation by secondary and backscattered electrons from microtomed and stained surface", Polymer, 34, 253-256(1993)

36. K. Premphet and W. Paecharoenchai, "Polypropylene / Metallocene ethylene-octene copolymer blends with a bimodal particle size distribution: mechanical properties and their controlling factors", J. Appl. Polym. Sci., 85, 2412-2418 (2002)

37. A.K. Kalkar, H.W. Siesler, F. Pfeifer, S.A. Wadeka, "Molecular orientation and relaxation in poly(butyleneterephthalate)/polycarbonate blends", Polymer, 44, 7251–7264 (2003)

38. B. Chisholm, "Blends of amide-modified polybutylene terephthalate and polycarbonate", SPE ANTEC Technical Papers, 2508-2514 (1998)

39. C. Rauwendaal, "Polymer Extrusion", 4th Edition, Hanser Gardner Publications, USA (2001)

40. L. A. Utracki, "Polymer Blends Handbook", Kluwer Academic Publishers, Boston, USA (2002)

41. C. J. Rauwendaal, "Analysis and experimental evaluation of twin screw extruders", Polym. Eng. Sci., 21, 1092-1100 (1981)

42. C. D. Denson, B. K. Hwang Jr., "The influence of the axial pressure gradient on flow rate for Newtonian liquids in a self wiping, co-rotating twin screw extruder", Polym. Eng. Sci., 20, 965-971(1980)

43. R. M. Secor, "Power consumption of partially filled twin-screw extruders", Polym. Eng. Sci., 26, 969-973 (1986)

44. H. E. H. Meijer, P. H. M. Elemans, "The Modeling of Continuous Mixers. Part I: The Co-rotating Twin-Screw Extruder", Polym. Eng. Sci., 28 , 275-290 (1988)

45. J. Gao, G. C. Walsh, D. Bigio , R. M. Briber, Mark D. Wetzel , "Mean residence time analysis for twin screw extruders" , Polym. Eng. Sci. , 40, 227-237 (2000)

46. A. Kumar, S. A. Eker, P.K. Houpt, "A model based approach for estimation and control for polymer compounding ", IEEE, 1, 729 – 735 (2003)

47. Z. Linjie, G. Xiaozheng, " Physical model of polymer pellets melting in co-rotating twin-screw extruder", SPE ANTEC Technical Papers, 149-153 (2000)

48. A. Shah and M. Gupta, "Comparison of the flow in co-rotating and counter- rotating twin-screw extruders", SPE ANTEC Technical Papers, 443-447 (2004)

49. A. A. Collyer, "Techniques in Rheological Measurements", Chapman & Hall, UK (1993)

50. D. E. D. Laney, J. F. Reilly, "A Practical Approach to Polymer Rheology for Quality Control", SPE ANTEC Technical Papers, 1162-1166 (1999)

51. A. V. Shenoy, D. R. Saini, "Melt Flow Index: More Than Just A Quality Control Rheological Parameter. Part I", Adv. Polym. Tech. , 6, 1-58 (1986)

52. C. W. Macosko, "RHEOLOGY : Principle, Measurements, and Applications", VCH Publishers Inc. , New York, 1994

53. Xu, Z. Hou and T. Li , "Novel Sample Preparation Method of Polymer Emulsion for SEM Observation", Microscopy Research and Technique, 70, 847–850 (2007)

54. S. Y. Hobbs and **V.** H. Watkins, "The Use of Chemical Contrast in the SEM Analysis of Polymer Blends", J. Polym. Sci. : Polym. Phys. Ed. , 20, 651-658 (1982)

55. L. M. Robeson, "Polymer Blends : A comprehensive Review", Hanser Gardner Publications, Canada (2007)

56. L. M. Berkowitz and P. N. Rylander, "Use of Ruthenium Tetroxide as a Multi-purpose Oxidant", J. Amer. Chem. Soc. , 80, 6682-6684 (1958)

57. Ancheh, V. N. , "A Study of Polycarbonate / Poly (butylene terephthalate) Compounding in a Twin Screw Extruder", Masters Dissertation, University of Waterloo, Waterloo, Ontario, Canada (2008)

58. R. M. Schulken, R. H. Cox and L. A. Minnick, "Dynamic and Steady-State Rheological Measurements on Polymer Melts", J. Appl. Polym. Sci. , 25, 1341-1353 (1980)

59. T. T. Hsieh, C. Tiu and G. P. Simon, "Melt Rheology of Aliphatic Hyperbranched Polyester with Various Molecular Weight", Polymer, 42, 1931-1939 (2001)

60. H. C. Booij, P. Leblans, J. Palmen, G. T-Thoone, "Nonlinear viscoelasticity and the Cox-Merz relations for polymeric fluids", J. Polym. Sci.: Polym. Phys. Ed.,. 21, 1703-1711 (1983)

61. J. Wu, Y. W. Mai and A. F. Yee, D. Yu, "Fracture toughness and fracture mechanisms of PBT/PC/IM blends", J. Mater. Sci., 29, 4510-4522 (1994)

62. J. S. Trent, J. I. Scheinbeim and P. R. Couchman, "Ruthenium Tetraoxide Staining of Polymers for Electron Microscopy", Macromolecules, 16, 589-598 (1983)

APPENDIX

Experimental Graphs

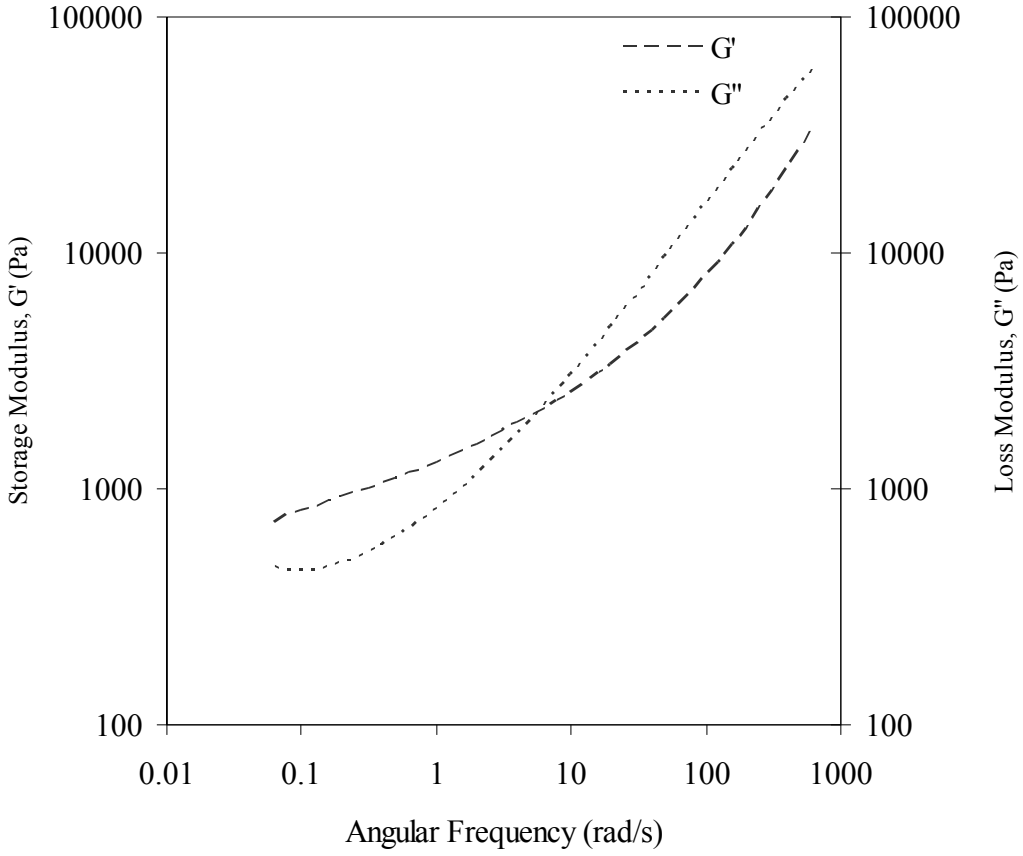

Fig. A.1 : Dynamic response behaviour of PC/PBT blends of 1st set of experiments of Run6

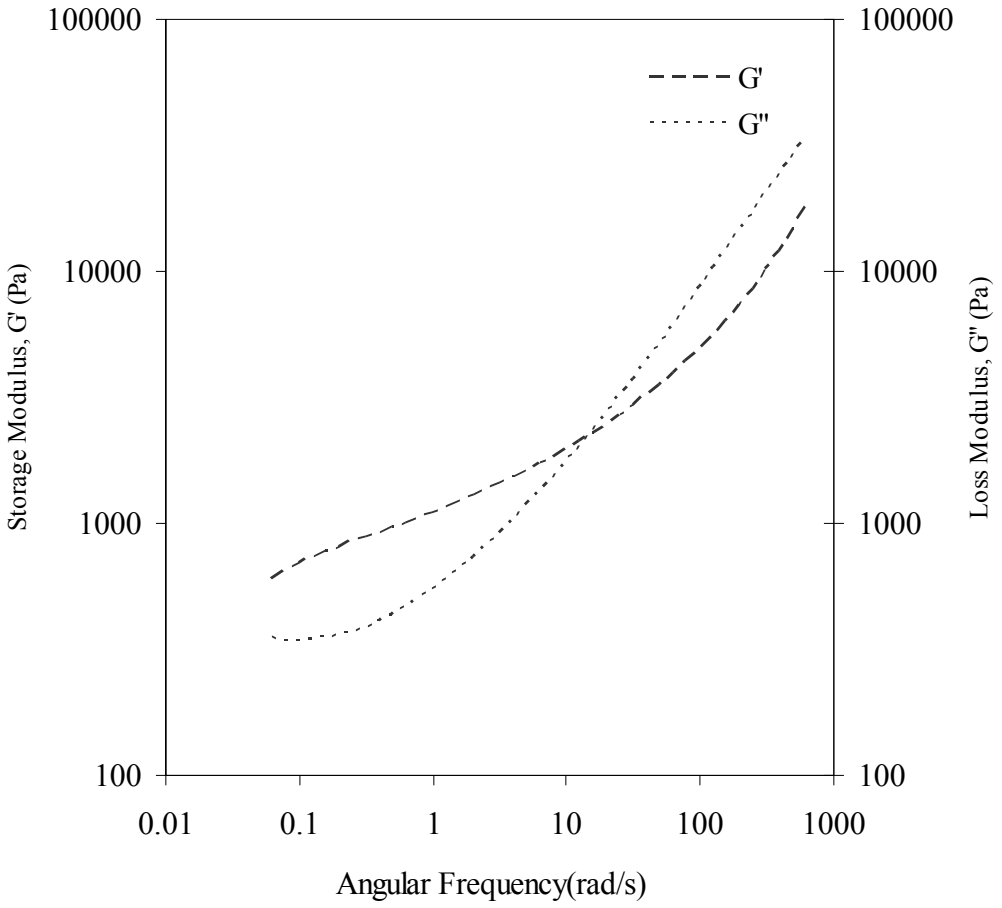

Fig. A.2 : Dynamic response behaviour of PC/PBT blends of 1st set of experiments of Run13

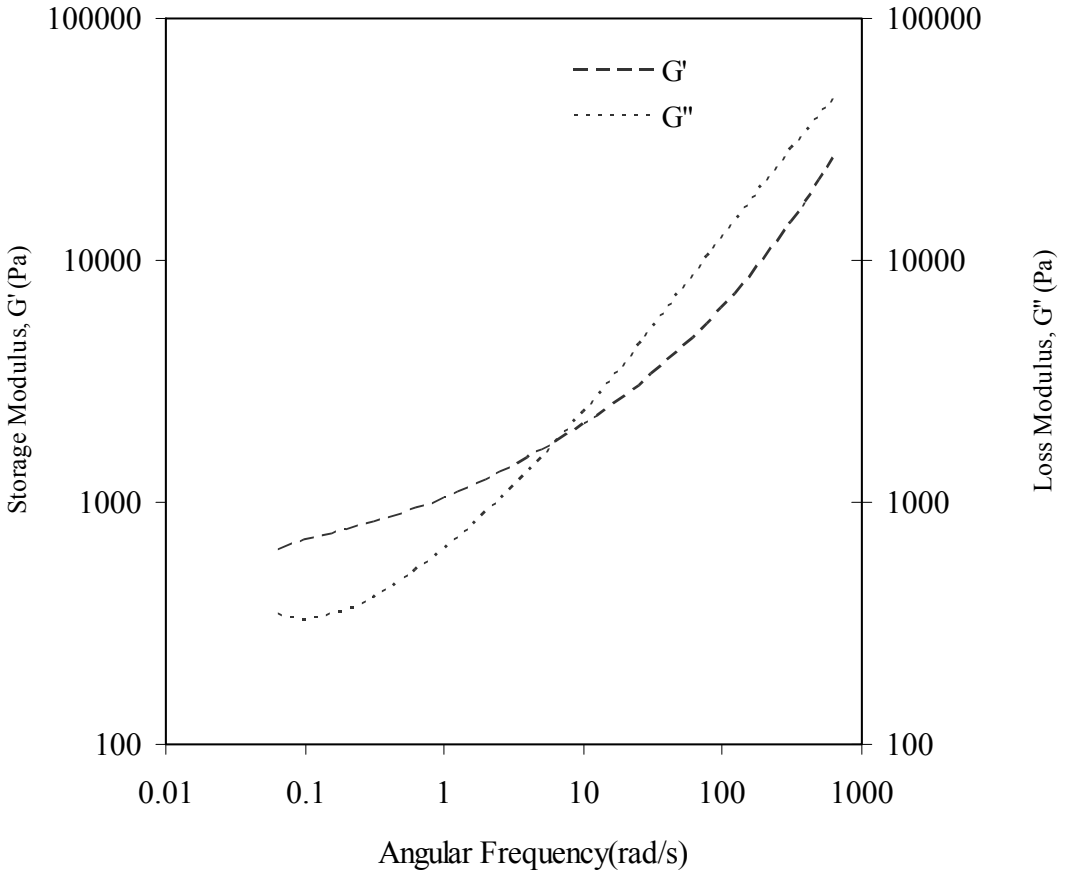

Fig. A.3 : Dynamic response behaviour of PC/PBT blends of 2nd set of experiments of Run7

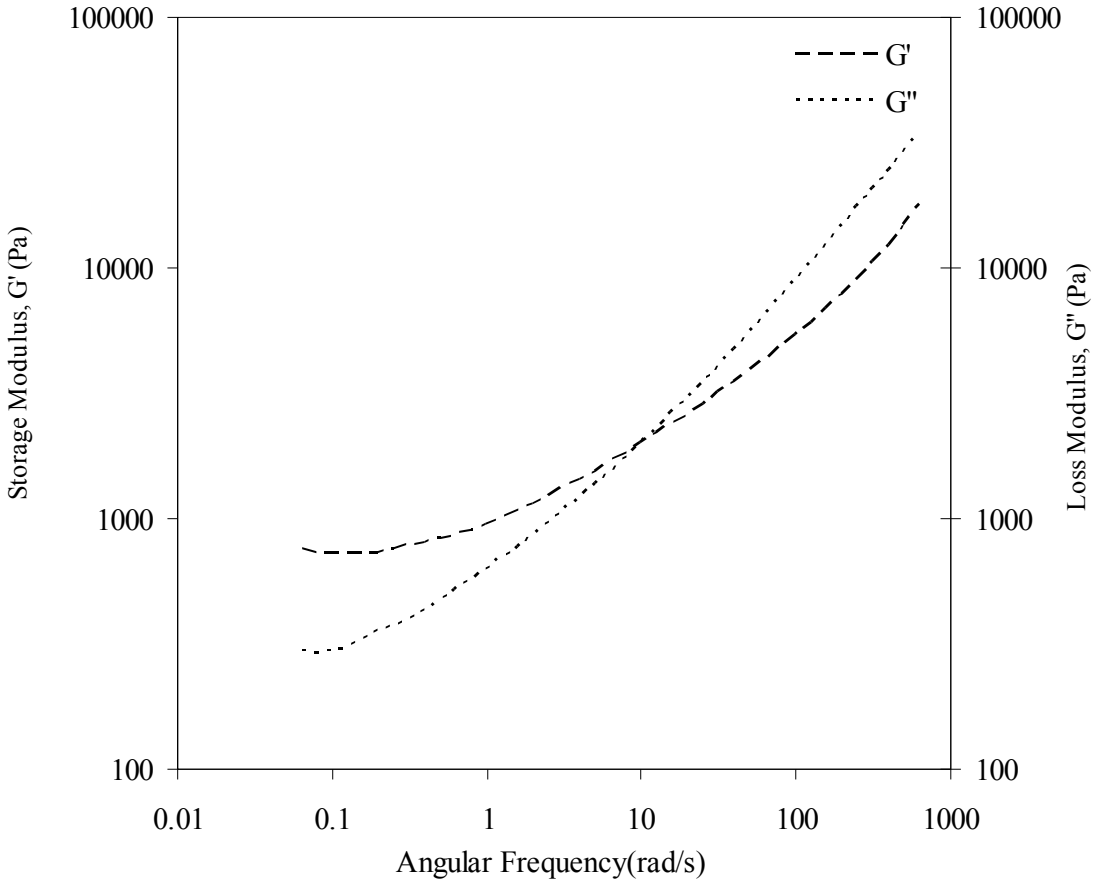

Fig. A.4 : Dynamic response behaviour of PC/PBT blends of 2nd set of experiments of Run13

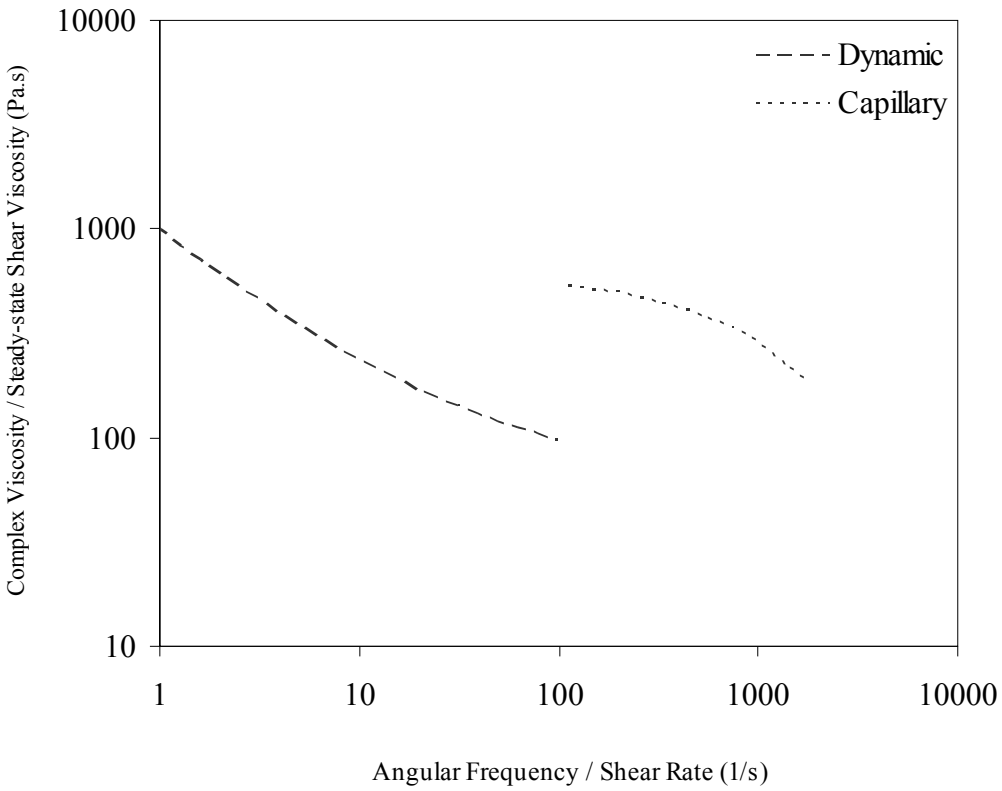

Fig. A.5: Complex Viscosity / Steady-shear Viscosity as a function of Angular Frequency / Shear Rate for Run9 of the 2nd set of experiments.

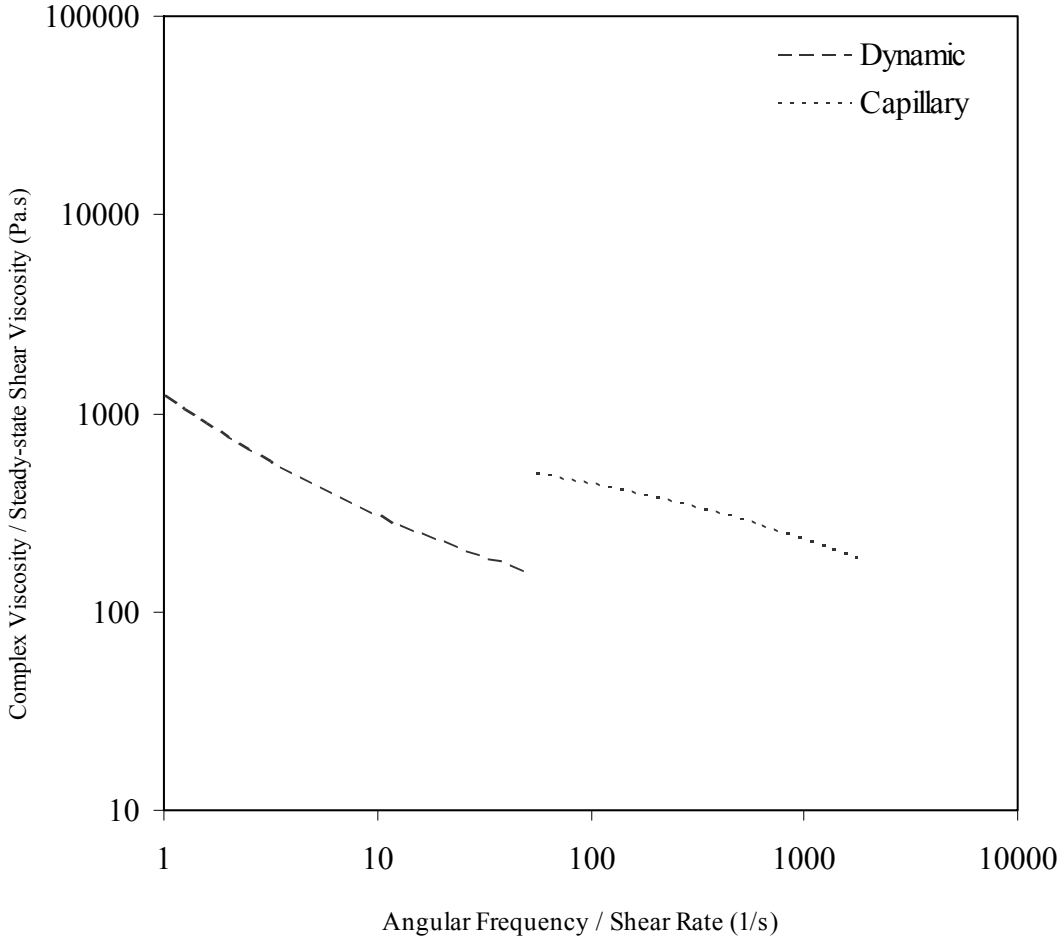

Fig. A.6 : Complex Viscosity / Steady-shear Viscosity as a function of Angular Frequency / Shear Rate for Run11 of the 2nd set of experiments.

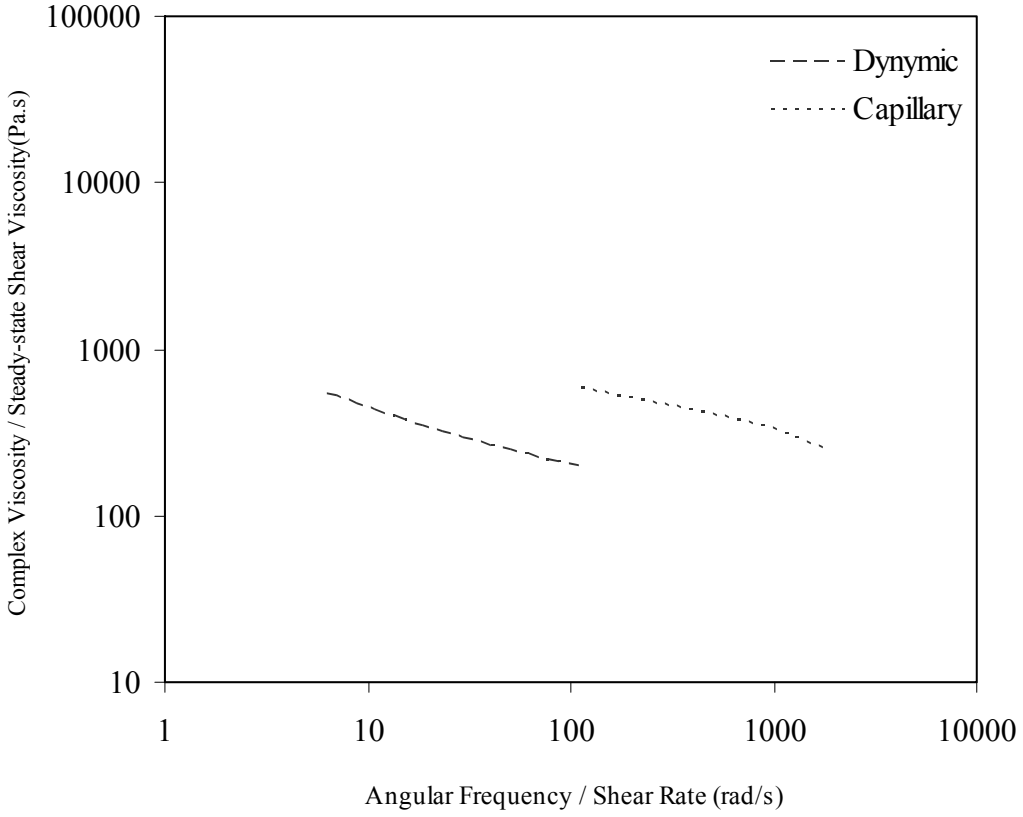

Fig. A.7 : Complex Viscosity / Steady-shear Viscosity as a function of Angular Frequency / Shear Rate for Run5 of the 3rd set of experiments.

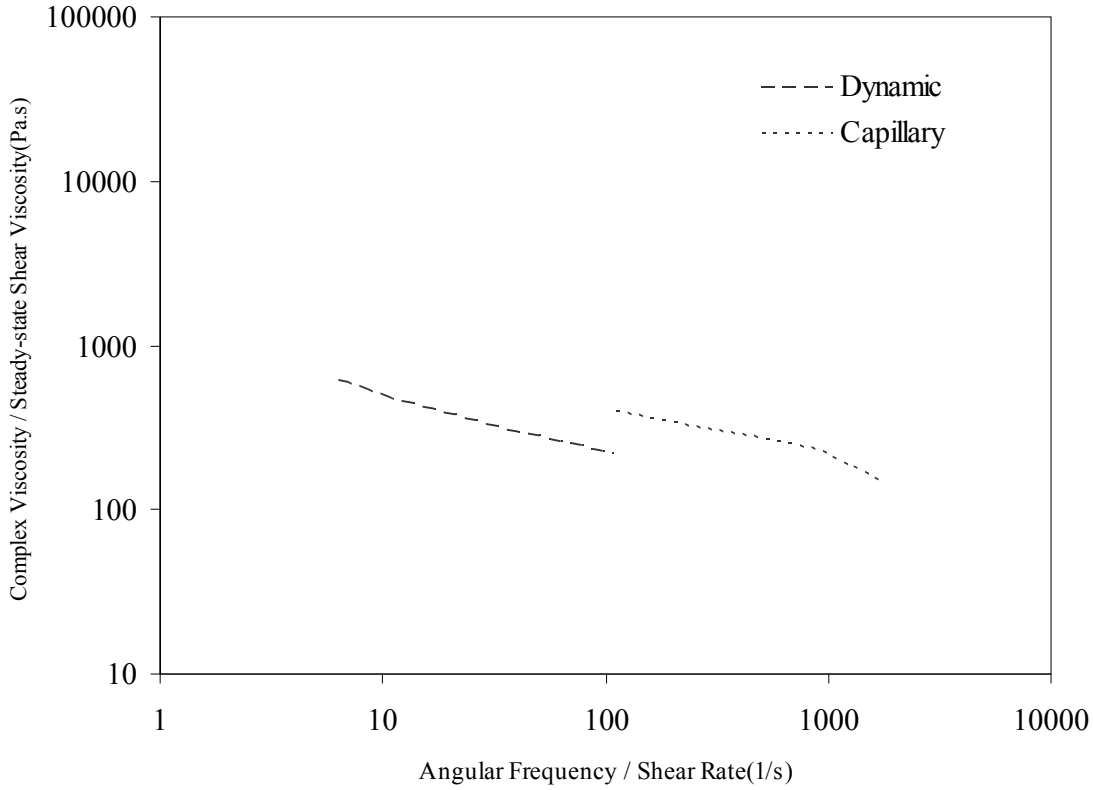

Fig. A.8 : Complex Viscosity / Steady-shear Viscosity as a function of Angular Frequency / Shear Rate for Run7 of the 3rd set of experiments.